

國立臺灣大學理學院物理學系

碩士論文

Department of Physics

College of Science

National Taiwan University

Master Thesis

開放量子系統下量子邏輯閘的最佳化控制

Optimal Control of Quantum Gate Operations in

Open Quantum Systems



黃琮暉

Tsung-Wei Huang

指導教授：管希聖 博士

Advisor: Hsi-Sheng Goan, Ph.D.

中華民國 98 年 7 月

July, 2009

誌謝

此篇碩士論文能順利完成，首先感謝我的指導教授管希聖博士，謝謝您這段時間來的教導，給予我論文著手的方向。從您身上學會做研究應有的態度。另外特別感謝蘇正耀教授周忠憲教授兩位口試委員，百忙之中抽空來參加我的口試，並且給予我許多研究上的建議。

感謝 501 所有一起奮鬥的學長、同學。室長陳柏文學長，在我有學術上的問題，他總是能提供建議或是書籍讓我省下不少的時間。劉彥甫學長，501 的大好人，在我們士氣最低落或是下大雨需要專車接送的時候，他會開著車載著我們去兜風放鬆心情。黃上瑜學長，當程式出問題的時候，他絕對是最佳幫手。吳致盛同學，501 的 google 天王，所有的問題，諸如論文排版或是其他問題，他都能用最快速度在網路上找到答案。柯百謙同學，一起出生入死的好兄弟，總是會於開完會後相約在陽台上一同喝著飲料，聊著未來。冷智群同學，擁有海豚音的男人，在 KTV 都是我們的走音救星。陳哲明同學，公館小明魔術師，總在最累的時候跳出來娛樂大家，讓我們在歡樂聲中度過。另外也感謝其他不是 501 的朋友，耿銘學長、安良學長、香綺、汝萱、思涵、岱沂等朋友不管在學業上或是生活上的幫忙或照顧。

另外，還要感謝我的父母親，如果沒有他們這麼多年來的栽培、付出，我要熬到碩士畢業是不可能的，他們常辛苦的繞過蘇花公路來到台北看我，這樣的親情與對我的愛護，實在無法用言語表達我對他們的感謝與愛。最後，感謝我的女友雅鈞，她永遠在我的背後支持著我，雖然因為忙碌的關係無法常常見面，他依舊是我可以熬過這兩年碩士生涯的動力來源。每天透過電話的互相安慰一直是我期待的時間，真的很感謝她的忍耐與支持。

要感謝的人很多，掛一漏萬，若有遺漏在此也一併獻上內心最深的謝意。

摘要

擁有操作時間遠快於去相干化(decoherence)時間的通用(universal set)量子邏輯閘是實行量子電腦最重要的限制條件之一。除此之外，符合錯誤限制條件(大約 $10^{-3} \sim 10^{-4}$)的高度準確度量子邏輯閘(quantum gates)，對於發展可容錯的量子計算(fault-tolerant quantum computation)也是極於需要的。在這篇論文中，我們使用科羅托夫(Kroto)方法，在肯恩(Kane)的矽基底施子自旋量子電腦系統(silicon-based donor spin quantum computer，其中我們以予體電子自旋當做量子位元(qubit))中，找到接近最佳化時間的高準確度(high-fidelity)量子邏輯閘的控制序列。首先，我們回顧肯恩的矽基底施子自旋量電腦系統，如何控制及構成量子邏輯閘，包括：阿達馬邏輯閘(Hadamard gate)、受控制否邏輯閘(CNOT gate)等等。其次，我們介紹科羅托夫最佳化方法，在電腦模擬中，這是一種最有效解決大維度向量空間最佳化控制問題的方法。之後，我們利用科羅托夫方法應用於肯恩的矽基底予體電子自旋量子，由此找出阿達馬邏輯閘的最佳化控制序列。在實現量子電腦的事件中，量子去相干化依舊是最主要的障礙。因此，我們考慮去相干的模型，利用主方程式(master equation)導出量子位元的運動方程式，進而構成量子邏輯閘在外加(熱庫)環境演化的運動方程式。最後，我們利用科羅托夫方法找出阿達馬邏輯閘在外加環境影響下的最佳化控制序列。

Abstract

One of the important criteria for physical implementation of a practical quantum computer is to have a universal set of quantum gates with operation times much faster than the relevant decoherence time of the quantum computer. In addition, high-fidelity quantum gates to meet the error threshold of about $10^{-3} \sim 10^{-4}$ are also desired for fault-tolerant quantum computation. So the main purpose of this thesis is to focus on finding control parameter sequence in near time-optimal way using an optimization approach, the Krotov method, for high-fidelity quantum gates in the Kane silicon-based donor spin quantum computer architecture where the donor electron spins are defined as quantum bits (qubits). We first review the basics of silicon-based donor spin quantum computer proposed by Kane, and how to control the system and construct the quantum gates, including Hadamard gate, CNOT gate and so on, in canonical gate decomposition ways. We then introduce the Krotov optimization method which is one of the most effective and universal computation methods for solving optimal control problems with a large dimension of state vectors. The Krotov method is then applied to find the optimal control sequence of a Hadamard gate in the Kane quantum donor electron spin computer. Quantum decoherence is still a major obstacle for the implementation of a practical quantum computer. We then consider a decoherence model, derive a corresponding quantum master equation of the reduced density matrix of the qubits, and construct equations of motion for quantum gate evolution in the presence of external (thermal) environments. Finally, we apply the Krotov method to find optimal control sequence for Hadamard gate operation under the influence of external environments.

Contents

| | | |
|----------|--|-----------|
| 1 | Introduction | 1 |
| 2 | Silicon-base donor spin Quantum Computer | 3 |
| 2.1 | Kane Quantum Computer Architecture and Hamiltonian | 3 |
| 2.2 | The Reduced Hamiltonian | 7 |
| 2.2.1 | Singel Qubit | 7 |
| 2.2.2 | Two-qubit system | 8 |
| 3 | Global Methods:Krotov Method | 10 |
| 3.1 | Preliminary Description of The Problem | 10 |
| 3.2 | The Basic Idea of Krotov Method | 11 |
| 3.2.1 | Decomposition and Definitions | 11 |
| 3.2.2 | The iterative algorithm of Krotov method | 12 |
| 3.3 | Construction of ϕ | 14 |
| 3.3.1 | First Order In x | 14 |
| 3.3.2 | Second Order in x | 16 |
| 3.3.3 | Algorithm | 17 |
| 3.4 | Discrete time interval system | 17 |
| 3.5 | Examples | 18 |
| 3.5.1 | Discrete variant | 18 |
| 3.5.2 | The Continuous in Time System With One Equation of Motion | 19 |
| 4 | Quantum system with Environment | 23 |

| | | |
|----------|---|-----------|
| 4.1 | Master Equation | 23 |
| 4.1.1 | Density Matrix | 23 |
| 4.1.2 | Derivation of Master Equation | 24 |
| 4.1.3 | Born Approximation | 27 |
| 4.1.4 | Markovian Approximation | 28 |
| 4.2 | Master Equation for a Two-Level System | 30 |
| 4.2.1 | Thermal Equilibrium | 30 |
| 4.2.2 | Dephasing | 33 |
| 5 | Optimal Control in Open Quantum Systems | 35 |
| 5.1 | Introduction | 35 |
| 5.2 | Krotov Method in Density Matrix | 36 |
| 5.2.1 | Equation of Motion | 36 |
| 5.2.2 | Goal Functional | 38 |
| 5.2.3 | Decompose the goal functional in Quantum System | 39 |
| 5.3 | In Silicon-base Donor Spin Quantum Computer | 40 |
| 5.3.1 | System | 40 |
| 5.3.2 | Hadamard Gate | 43 |
| 5.4 | Result | 46 |
| 6 | Conclusion | 52 |
| | Bibliography | 54 |
| A | Changing a Matrix to a Column | 56 |

List of Figures

| | | |
|-----|--|----|
| 2.1 | The Kane quantum computer architecture | 4 |
| 2.2 | Energy levels of the donor electron-nucleus system obtained by using 2nd order approximation with a magnetic field B and hyperfine coupling A. | 6 |
| 3.1 | Optimal evolution of x for different numbers of iterations | 22 |
| 4.1 | Schematic picture of an open system | 24 |
| 5.1 | The symbol of the quantum circuit for Hadamard | 44 |
| 5.2 | The step for finding out the equation of motion for operator in real functional. | 45 |
| 5.3 | Relation of the optimal fidelity versus the gate operation time. The highest fidelity occur at the gate operation time of 12.35ns | 47 |
| 5.4 | Relation of iteration number and the fidelity. We pick the gate operation time of 12.16ns | 47 |
| 5.5 | The control sequence and the result from Krotov method | 48 |
| 5.6 | State probability evolution of the Hadamard gate for an initial state $ 1\rangle$ | 49 |
| 5.7 | State probability evolution of the Hadamard gate for an initial state $ 0\rangle$ | 49 |
| 5.8 | State probability evolution of the Hadamard gate for an initial state $\frac{1}{\sqrt{2}}(1\rangle + 0\rangle)$ | 50 |
| 5.9 | State probability evolution of the Hadamard gate for an initial state $\frac{1}{\sqrt{2}}(1\rangle - 0\rangle)$ | 51 |

List of Tables

| | | |
|-----|---|----|
| 2.1 | Typical parameters used for numerical calculations. | 9 |
| 3.1 | Evolution of functional with the iteration numbers. The iteration number is defnoted in "No." column. | 20 |



Chapter 1

Introduction

Quantum mechanics is more fundamental laws than classical. It makes us believe that the quantum computer could be done. In 1985, Deutsch [1].introduced the idea of a quantum computer that makes use of superposition, interference entanglement or other quantum effects based on the principles of quantum mechanics. In 1994, Shor presented his quantum factoring and discrete logarithm finding algorithms. In 1996, Grover published an quantum algorithm for searching an unordered database. These quantum algorithms can very substantially computational and make possible to solve those problems which are impossible or difficult to solve with classical computers. All of the quantum algorithms need a practical quantum computer to run and to achieve what we want to do. To construct a quantum computer, the first thing is to find a quantum system which has well-defined quantum bits and relatively long quantum coherence time and can make universal quantum gates. The universal quantum gate means that through the control of the system, if one can perform two qubit gate operations, such as CNOT-gate or \sqrt{SWAP} -gate, and all of the single-qubit gate operations then all other quantum gates can also be performed. Recently, the most notable physical systems for quantum computer proposals are the linear quantum optics, superconducting Josephson junction,ion trap,quantum dot, impurity in semiconductor and liquid state nuclear magnetic resonance(NMR). In this thesis, we study the proposal of the Kane silicon-based donor spin quantum computer introduced in chapter 2

An important requirement for a practical quantum computer is to have high-fidelity quantum gates with a operation time much shorter than the decoherence time. So to achieve a high-fidelity quantum gate operation in a shortest time is desired. This near time-optimal, high-fidelity control problem has attracted much attention recently. In this thesis, we will investigate quantum optimal control problem for Kane quantum computer using optimization method called the Krotov method [5] [6]. In some optimization methods, one may get stuck into local minima of the optimal control problem. However, the method developed by Krotov can obtain the global minimum result. The Krotov method can deal with almost all of the optimal control problems if the equations of motion of the system can be formulated. We will introduce this method in chapter 3.

In chapter 2 we describe the model for the Kane silicon-based donor spin quantum computer, but in real case we need to consider the system coupled to external environments. Therefore, in chapter 4 we will introduce the theory of open system using the master equation approach. Also, in chapter 4 we will use Born and Markov approximations. To obtain the master equation for a simple dephasing model which will be used in our system.

In chapter 5, we will apply the Krotov method to investigate the quantum optimal control problem for the quantum gate operations of the Kane quantum computer. We will first introduce how to apply the Krotov method in quantum system. We will then use the method to obtain optimal control sequence for a single qubit gate, Hadamard gate.

Chapter 2

Silicon-base donor spin Quantum Computer

2.1 Kane Quantum Computer Architecture and Hamiltonian

The silicon-based donor spin quantum computer was proposed by Kane [2] in 1998. The Kane computer satisfies the criteria that qubits can be identified, it is possible to prepare initial states and control these state, and the decoherence time is slow in comparison to typical gate speeds. Therefore, in principle, the Kane quantum computer satisfies all of the important requirements of a quantum computer. In the Kane quantum computer architecture, the phosphorous donor atoms are embedded in a Si crystal and arranged in a array. As a first approximation, four of five valence electrons of each ^{31}P atom bonds to neighboring Si atom, and the fifth electron forms a hydrogen-like S-orbital around each $^{31}\text{P}^+$ ion. In the original proposal of Kane, the nuclear spin of each phosphorous (^{31}P) represents a single qubit. Here we use the phosphorous donor electron spins as qubit. The schematic diagram of Kane quantum computer is shown in Fig. 2.1 Using the electrodes above and between each qubit and the global static and oscillating magnetic fields, one can achieve the control of each qubit. Using the formula of hydrogen-like atom, the Bohr radius and bound state

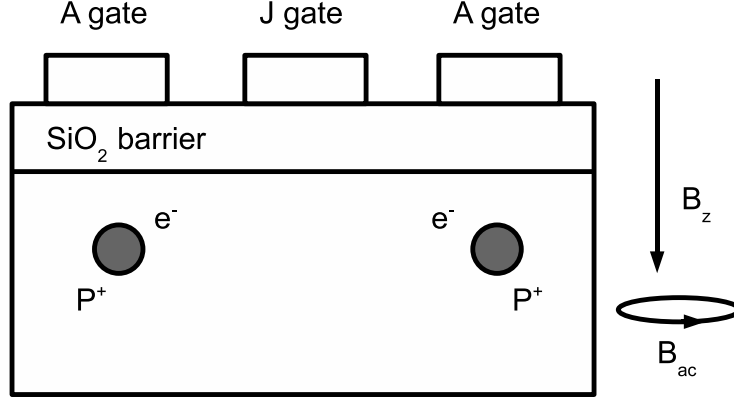


Figure 2.1: The Kane quantum computer architecture

energy levels can be estimated be:

$$a_B^* = \epsilon \frac{m_e}{m^*} a_B, \quad (2.1)$$

$$E_n = \frac{m^*}{\epsilon^2 m_e} E_n^H, \quad (2.2)$$

where $\epsilon = 11.7$ is the susceptibility of Si, and the effective mass $m^* \approx m_T^* = 0.27m_e$ (where m_e is the free electron mass, and m_T^* is the transverse effective mass in Si). Using the value of the Bohr radius and the bound state energies of a hydrogen atom : $a_B = 0.053\text{nm}$ and $E_n^H = -13.6\text{eV}/n^2$, we obtained effective $a_B^* \approx 2.3\text{nm}$ and $E_1 \approx -27\text{meV}$.

In the enough low temperatures (about milli-kelvin temperatures), the donor electron will only occupy the lowest energy bound state. Therefore, the electron donor will be in the 1st s-orbital and concentrated at the donor nucleus, getting a large hyperfine coupling energy. The strength, A , of the hyperfine interaction is proportional to the value of the donor electron wave-function evaluated at the nucleus,

$$A = \frac{8\pi}{3} \mu_B g_n \mu_n |\psi(0)|^2, \quad (2.3)$$

where μ_B is the Bohr magneton, and μ_n is the proton Bohr magneton. A typical strength for hyperfine interaction is $A = 1.2 \times 10^{-4}\text{meV}$. Applying a voltage on

'A' gates placed directly above each ^{31}P nucleus distort the shape of the electronic wavefunction thereby reducing the strength of the hyperfine coupling. The total effective single-qubit spin Hamiltonian including both hyperfine and Zeeman terms is given by:

$$H_B = -\frac{1}{2}g_n\mu_n B\sigma_Z^n + \frac{1}{2}g_e\mu_B B\sigma_Z^e + A\sigma_e \cdot \sigma_n, \quad (2.4)$$

where the effective g-factor of an electron in Si is $g_e = 2$, the g-factor for a ^{31}P nuclear spin is $g_n = 2.26$. Under the influence of a constant magnetic field B_0 in the z-axis, electron and nuclear spin will undergo a Larmor precession around the z-axis. But because of the hyperfine interaction, the electron and nuclear spin may flip. Because of the energy conservation and the Zeeman energy of the electron spin is about 1000 times larger than the nuclear, the probabilities that the electron and nuclear spins flip are very small. Therefore, if we initiate the nuclear spin in the lowest energy, spin-up state, we might change the effective Larmor precession frequency of a selected electron through tuning the hyperfine interaction strength achieved by applying a voltage on 'A' gate. Since the energy difference between the spin-up and spin-down state of the targeted electron could be controlled, the qubit can be selectively addressed.

To analyze the energy levels of the system, we diagonalize the Hamiltonian in Eq. (2.4). The Hamiltonian can be directly diagonalised. The eigen-energies are:

$$E_{|\uparrow_e\uparrow_n\rangle'} = \frac{1}{2}g_e\mu_B B_0 - \frac{1}{2}g_n\mu_n B_0 + A, \quad (2.5)$$

$$E_{|\uparrow_e\downarrow_n\rangle'} = \sqrt{\left(\frac{g_e\mu_B B_0 + g_n\mu_n B_0}{2}\right)^2 + 4A^2} - A, \quad (2.6)$$

$$E_{|\downarrow_e\uparrow_n\rangle'} = -\sqrt{\left(\frac{g_e\mu_B B_0 + g_n\mu_n B_0}{2}\right)^2 + 4A^2} - A, \quad (2.7)$$

$$E_{|\downarrow_e\downarrow_n\rangle'} = -\frac{1}{2}g_e\mu_B B_0 + \frac{1}{2}g_n\mu_n B_0 + A, \quad (2.8)$$

where the eigenstates are:

$$|\uparrow_e\uparrow_n\rangle' = |\uparrow_e\uparrow_n\rangle, \quad (2.9)$$

$$|\uparrow_e\downarrow_n\rangle' = \cos\left(\frac{\phi}{2}\right)|\uparrow_e\downarrow_n\rangle + \sin\left(\frac{\phi}{2}\right)|\downarrow_e\uparrow_n\rangle, \quad (2.10)$$

$$|\downarrow_e\uparrow_n\rangle' = -\sin\left(\frac{\phi}{2}\right)|\uparrow_e\downarrow_n\rangle + \cos\left(\frac{\phi}{2}\right)|\downarrow_e\uparrow_n\rangle, \quad (2.11)$$

$$|\downarrow_e\downarrow_n\rangle' = |\downarrow_e\downarrow_n\rangle, \quad (2.12)$$

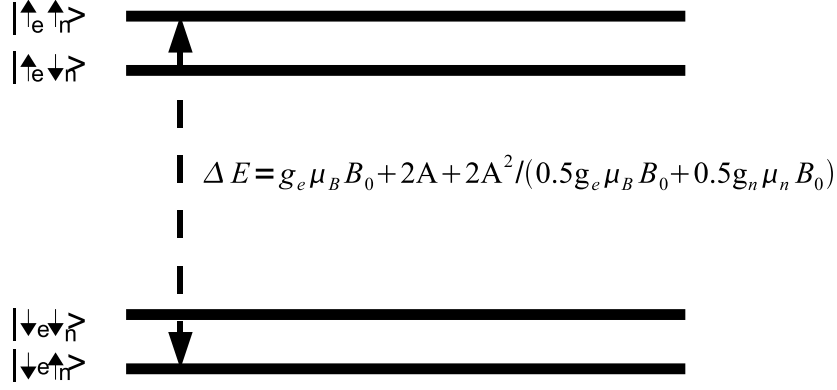


Figure 2.2: Energy levels of the donor electron-nucleus system obtained by using 2nd order approximation with a magnetic field B and hyperfine coupling A .

where $\phi = \tan^{-1} \left(\frac{2A}{\frac{1}{2}g_e \mu_B B_0 + \frac{1}{2}g_n \mu_n B_0} \right)$. Because of the hyperfine interaction, the eigenstates are not in the basis states: $|\uparrow_e \uparrow_n\rangle$, $|\uparrow_e \downarrow_n\rangle$, $|\downarrow_e \uparrow_n\rangle$ and $|\downarrow_e \downarrow_n\rangle$. However, the typical hyperfine interaction $2A$ is about 500 times smaller than the Zeeman energy, and we thus have $\phi \approx 0$. Therefore, we can use the perturbation theory to treat the small hyperfine interaction. By using the second order perturbation theory, the energy level are given as follows:

$$E_{|\uparrow_e \uparrow_n\rangle} = \frac{1}{2}g_e \mu_B B_0 - \frac{1}{2}g_n \mu_n B_0 + A, \quad (2.13)$$

$$E_{|\uparrow_e \downarrow_n\rangle} = \frac{1}{2}g_e \mu_B B_0 + \frac{1}{2}g_n \mu_n B_0 - A + \frac{2A^2}{\frac{1}{2}g_e \mu_B B_0 + \frac{1}{2}g_n \mu_n B_0}, \quad (2.14)$$

$$E_{|\downarrow_e \uparrow_n\rangle} = -\frac{1}{2}g_e \mu_B B_0 - \frac{1}{2}g_n \mu_n B_0 - A - \frac{2A^2}{\frac{1}{2}g_e \mu_B B_0 + \frac{1}{2}g_n \mu_n B_0}, \quad (2.15)$$

$$E_{|\downarrow_e \downarrow_n\rangle} = -\frac{1}{2}g_e \mu_B B_0 + \frac{1}{2}g_n \mu_n B_0 + A. \quad (2.16)$$

A schematic picture is shown in Fig.(2.2)

2.2 The Reduced Hamiltonian

2.2.1 Singel Qubit

If the nuclear spin is up and apply a constant magnetic field B_0 , then the energy difference between electron spin-up and -down state form Eq.(2.13) and Eq. (2.15) is given in A by:

$$\Delta E(A) = g_e \mu_B B_0 + 2A + \frac{2A^2}{\frac{1}{2}g_e \mu_B B_0 + \frac{1}{2}g_n \mu_n B_0}. \quad (2.17)$$

By defining $w(A) = \Delta E(A)/\hbar$, then we can write the effective Hamiltonian, $H = (\hbar/2)w(A)\sigma_z^e$. If now we applied a rotations magnetic field rotating in the x-y plant, with the frequency of w_{ac} , the effective Hamiltonian will become :

$$H = \frac{\hbar w(A)}{2}\sigma_z + \frac{1}{2}g_e \mu_B B_{ac}(\cos(w_{ac}t)\sigma_x + \sin(w_{ac}t)\sigma_y). \quad (2.18)$$

To understand the control processes, we change to the frame rotating with the rotating magnetic field. It means:

$$\tilde{\rho} = U_{rot}\rho U_{rot}^\dagger, \quad (2.19)$$

where

$$U_{rot} = e^{\frac{i}{2}w_{ac}\sigma_z t}. \quad (2.20)$$

Inserting both Eq.(2.19)and Eq.(2.20) into Liouville-Von Neumann equation $\dot{\rho} = -\frac{i}{\hbar}[H, \rho]$ and use the identity $e^{\frac{i}{2}w_{ac}\sigma_z t}(\cos(w_{ac}t)\sigma_x + \sin(w_{ac}t)\sigma_y)e^{-\frac{i}{2}w_{ac}\sigma_z t} = \sigma_x$. We can get the reduced Hamiltonian in the rotating frame as:

$$\tilde{H} = \frac{\hbar}{2}(w(A) - w_{ac})\sigma_z + \frac{1}{2}g_e \mu_B B_{ac}\sigma_x. \quad (2.21)$$

We tune the angular frequency of rf magnetic field B_{ac} to the electron spin resonance frequency obtained when no voltage is applied to the corresponding A gate, that is $w_{ac} = w(A_0)$. If we define $\Delta w = w(A) - w(A_0)$, then the qubits will effectively rotate around the x-axis when $\Delta w = 0$ or equivalently $A = A_0$, and around an axis which is slightly shifted with respect to this axis , $\Delta w \neq 0$, described by Eq.(2.21).

2.2.2 Two-qubit system

The spins of the two adjacent electrons are coupled via the exchange energy J . The exchange energy contribution to the Hamiltonian is

$$H_J = J\sigma_{e_1} \cdot \sigma_{e_2}, \quad (2.22)$$

where e_1 and e_2 are two adjacent electrons. The strength of the exchange interaction can be approximated using the Herring-Flicker approximation [4].

$$J(a^*, d) \approx \frac{1.6e^2}{\hbar\epsilon a^*} \left(\frac{d}{a^*}\right)^{5/2} \exp\left(-\frac{2d}{a^*}\right), \quad (2.23)$$

which is valid when the inter-donor spacing, d , is much greater than the effective Bohr radius, a^* . The exchange interaction drops off exponentially, and is thought of as a short range interaction. We can change the voltage on the J gate to increase or decrease the exchange energy (applying positive voltage will increase the exchange energy, conversely, negative voltage will decrease). In a typical Kane quantum computer's scheme, the typical value of J is 4.23×10^{-5} eV that requires the separation between two neighboring donors is roughly 10-20nm that sets a stringent fabrication condition to fabricate surface A and J gate within such a short distance.

The full two qubit Hamiltonian in the static and oscillating magnetic fields can be written as

$$\begin{aligned} H = & \frac{1}{2}g_e\mu_B B_0(\sigma_z^{1e} + \sigma_z^{2e}) - \frac{1}{2}g_n\mu_n B_0(\sigma_z^{1n} + \sigma_z^{2n}) \\ & + \frac{1}{2}g_e\mu_B B_{ac}(\cos(w_{act})(\sigma_x^{1e} + \sigma_x^{2e}) + \sin(w_{act})(\sigma_y^{1e} + \sigma_y^{2e})) \\ & - \frac{1}{2}g_n\mu_n B_{ac}(\cos(w_{act})(\sigma_x^{1n} + \sigma_x^{2n}) + \sin(w_{act})(\sigma_y^{1n} + \sigma_y^{2n})) \\ & + A_1\sigma^{1e} \cdot \sigma^{1n} + A_2\sigma^{2e} \cdot \sigma^{2n} + J\sigma^{1e} \cdot \sigma^{2e}. \end{aligned} \quad (2.24)$$

Because the rotating operator U_{rot} of Eq.(2.20) commutes with the exchange interaction Hamiltonian H_J , the effective reduced two qubits Hamiltonian with the exchange interaction in the rotating frame can be similarly found and written as

$$\tilde{H} = \frac{\hbar}{2}\Delta w_1\sigma_z^1 + \frac{\hbar}{2}\Delta w_2\sigma_z^2 + \frac{1}{2}g_e\mu_B B_{ac}(\sigma_x^1 + \sigma_x^2) + J\sigma^{1e} \cdot \sigma^{2e}. \quad (2.25)$$

| Description | Term | Typical Value |
|---|----------------------------|--|
| Planck Constant ($\frac{\hbar}{2\pi}$) | \hbar | $6.58211889(26)\times 10^{-16}$ eVs |
| Electron Mass | m_e | $9.10938188(72)\times 10^{-31}$ kg |
| Proton Mass | m_n | $1.67262158(13)\times 10^{-27}$ kg |
| Elementary Charge | e | $1.602176462(63)\times 10^{-19}$ C |
| Bohr Magnetron | μ_B | $5.788381749(43)\times 10^{-5}$ eV T ⁻¹ |
| Proton Bohr Magnetron | μ_n | 3.15251241×10^{-8} eV T ⁻¹ |
| Electron g-factor | g_e | 2.0023193043737(82) |
| Effective Proton g-factor in Si | g_n | 2.26 |
| Unperturbed Hyperfine Interaction | A_0 | 1.211×10^{-7} eV |
| Minimum Varied Hyperfine Interaction | A_p | 0.606×10^{-7} eV |
| Constant Magnetic Field Strength | B_0 | 2.0 T |
| Electron Zeeman Energy ($\frac{1}{2}g_e\mu_B B_0$) at B_0 | | $1.159018851\times 10^{-4}$ eV |
| Nuclear Zeeman Energy ($\frac{1}{2}g_n\mu_n B_0$) at B_0 | | $7.124539805\times 10^{-8}$ eV |
| Maximum Exchange Interaction | J | 8.3×10^{-8} eV |
| Energy Difference in Reduced Hamiltonian | $\frac{\hbar}{2}w\sigma_z$ | -6.065×10^{-8} eV |

Table 2.1: Typical parameters used for numerical calculations.

We will use the reduced Hamiltonian to obtain an optimal control parameter sequence for quantum gate operations of the Kane donor electron spin quantum computing.

Chapter 3

Global Methods:Krotov Method

3.1 Preliminary Description of The Problem

Krotov method [5][6] is one of the most effective universal methods for solving optimal control problems with a large dimension of the state vectors to be of the order of $10^4 \approx 10^5$. So, it may one of the most appropriate and powerful method for solving optimal control problems of quantum systems. In the Krotov method, we just need to know the equation of motion of a system, and then we can find out the minima of "the goal functional" which depend on the system and the control. Consider the equation of motion of a system

$$\frac{dx}{dt} = f[t, x(t), u(t)]; \quad (3.1)$$

and suppose we want to minimize functional

$$I[x(t), u(t)] = \int_0^T f^0(t, x(t), u(t))dt + F[x(T)] \rightarrow \min; \quad (3.2)$$

Here $x(t)$ means the system evolution with time or the trajectory, $u(t)$ is control value with time, and the vector-functional $f[t, x(t), u(t)]$ and the functional $F[x(t)]$ are defined for all $t, x(t), u(t)$ and are twice differentiable with respect to t and x . The initial vector $x(0) = \xi$ is a given and fixed vector, $x(T)$ is final values of the vector $x(t)$, and u belong to a close set U . Where $F[x(T)]$ and $f^0[t, x(t), u(t)]$ are general functionals that represent that I depends on the terminal and intermediate

time value of x . The general functional, $F[x(T)]$, only depends on the final value of $x(t)$, and $f^0[t, x(t), u(t)]$ depends on the intermediative values of $x(t)$ and $u(t)$.

For the quantum system or multiaraument processes, we will have more than one equation of motion, $\frac{dx^i}{dt} = f^i[t, x^i(t), u(t)]$, and the minimization problem will become to $I[t, x^i(t), u(t)] = \int_0^T f^0[t, x^i(t), u(t)]dt + F[x^i(T)]$, where $i = 1, 2 \dots n$.

3.2 The Basic Idea of Krotov Method

3.2.1 Decomposition and Definitions

We introduce a real, differentiable function $\phi[t, x(t)]$, and follow constructions:

$$R[t, x(t), u(t)] = \frac{\partial \phi}{\partial x} f[t, x(t), u(t)] - f^0[t, x(t), u(t)] + \frac{\partial \phi}{\partial t}, \quad (3.3)$$

$$G[T, x(T)] = F(T, x(T)) + \phi(T, x(T)), \quad (3.4)$$

$$L[x(t), u(t), \phi] = G[T, x(T)] - \int_0^T R[t, x(t), u(t)]dt - \phi[0, x(0)]. \quad (3.5)$$

It can be shown that for any function $\phi[t, x(t)]$ and all of $x(t)$ and $u(t)$, $L[x(t), u(t), \phi] = I[x(t), u(t)]$. The proof is shown as follows:

$$\begin{aligned}
L[x(t), u(t), \phi] &= G[T, x(T)] - \int_0^T R[t, x(t), u(t)]dt - \phi_0[x(0)] \\
&= F(T, x(T)) + \phi(T, x(T)) \\
&\quad - \int_0^T \left[\frac{\partial \phi}{\partial x} f[t, x(t), u(t)] - f^0[t, x(t), u(t)] + \frac{\partial \phi}{\partial t} \right] dt \\
&\quad - \phi[0, x(0)] \\
&= F(T, x(T)) + \phi(T, x(T)) \\
&\quad - \int_0^T \left[\frac{\partial \phi}{\partial x} \frac{dx}{dt} + \frac{\partial \phi}{\partial t} - f^0[t, x(t), u(t)] \right] dt \\
&\quad - \phi[0, x(0)] \\
&= F(T, x(T)) + \phi(T, x(T)) - \int_0^T \frac{d\phi}{dt} dt \\
&\quad + \int_0^T f^0[t, x(t), u(t)] dt - \phi(0, x(0)) \\
&= F(T, x(T)) + \int_0^T f^0[t, x(t), u(t)] dt \\
&= I[t, x(t), u(t)]. \tag{3.6}
\end{aligned}$$

Therefore, minimizing $I[t, x(t), u(t)]$ can be achieved by minimizing $L[t, x(t), u(t), \phi]$, and this means to minimizing $G[x(T)]$ and maximizing $R[t, x(t), u(t)]$.

For the quantum system or multiraument processes, the equationals of R and G will become to $R[t, x^i(t), u(t)] = \frac{\partial \phi}{\partial x^i} f^i[t, x^i(t), u(t)] - f^0[t, x^i(t), u(t)] + \frac{\partial \phi}{\partial t}$ and $G[T, x^i(T)] = F[T, x^i(T)] + \phi[T, x^i(T)]$. It is convenient for later to define the function $\Phi = \frac{\partial \phi}{\partial x^i}$, and the functional $R[t, x^i(t), u(t)] = H[t, x(t), u(t), \Phi(t)] + \frac{\partial \phi}{\partial t}$, where

$$H[t, x^i(t), u(t), \Phi(t)] = \Phi f(t, x^i(t), u(t)) - f^0[t, x^i(t), u(t)]. \tag{3.7}$$

Note the parameter in H denoted by Φ , which emphasizes that x^i and $\frac{\partial \phi}{\partial x}$ should be treated as independent variables, with respect to H .

3.2.2 The iterative algorithm of Krotov method

The main goal of Krotov method is to find out a series of control, $u_s(t)$, to make the value of the goal functional $I[t, x(t), u(t)]$ become a monotonically decreasing function, $I[t, x_s(t), u_s(t)] < I[t, x_{s+1}(t), u_{s+1}(t)]$. The main idea is that because we

can be completely free in choosing the functional $\phi[t, x(t)]$, if we can construct the functional $\phi[t, x(t)]$ to make the series of $L_s[t, x(t), u(t), \Phi(t)]$ being maximized, in each s , then, when we randomly choose next $u_{s+1}(t)$, without worrying about the effect of $u(t)$ on $L[t, x(t), u(t), \Phi]$, we will get a smaller value of the goal functional.

Suppose that we have already found out the construction of the functional $\phi[t, x(t)]$. Then the optimal process will be as follows:

(1) We begin by taking an arbitrary control history $u^0(t)$ and the corresponding trajectory $x^0(t)$ (3.1).

(2) The functional $\phi[t, x(t)]$ makes $L[t, x(t), u(t), \Phi(t)]$ a maximum at this control $u^0(t)$ and trajectory $x^0(t)$. This is equivalent to the following two conditions:

$$R[t, x^0(t), u^0(t)] = \min_x R[t, x(t), u^0(t)]. \quad (3.8)$$

$$G[T, x(T)] = \max_x G[T, x(T)]. \quad (3.9)$$

These conditions mean that the functionals R and G are calculated using the new $\phi[t, x(t)]$. Therefore, the current $x^0(t)$ will be the worst of all possible $x(t)$'s in minimizing the goal functional $L[t, x(t), u(t), \Phi] = I[t, x(t), u(t)]$. Any change in $u(t)$ which makes a new trajectory $x(t)$ will now only improve the minimization of goal function $I[t, x(t), u(t)]$.

(3) We can find a control $u(t)$ denoted by \tilde{u} that maximizes the functional, H (3.7). The \tilde{u} corresponds the condition:

$$\begin{aligned} \tilde{u}(t, x(t)) &= \arg \max_u H[t, x(t), u(t), \Phi]. \\ &= \arg \max_u R[t, x(t), u(t)]. \end{aligned} \quad (3.10)$$

Be careful that the control $\tilde{u}(t, x(t))$ depends on the function of the trajectory $x(t)$.

(4) The \tilde{u} needs to satisfy the equation of motion (3.1), so we can get the new history of control $u^1(t)$ and the new trajectory $x^1(t)$ by using the equation of motion.

(5) It is now guaranteed that minimization of the goal functional (3.2) has been improved, $I[t, x^1(t), u^1(t)] < I[t, x^0(t), u^0(t)]$. The new history of the control and the trajectory become a starting point of the next iteration and repeating 1-4 can achieve further decrease in the goal functional.

Next, we prove that the new $I[t, x^1(t), u^1(t)]$ indeed smaller than the old $I[t, x^0(t), u^0(t)]$. Because, the equation (3.6) that

$$I[t, x^0(t), u^0(t)] - I[t, x^1(t), u^1(t)] = L[t, x^0(t), u^0(t); \Phi] - L[t, x^1(t), u^1(t); \Phi] \quad (3.11)$$

Therefore,

$$\begin{aligned} L[t, x^0(t), u^0(t); \Phi] &- L[t, x^1(t), u^1(t); \Phi] \\ &= G[T, x^0(T)] - G[T, x^1(T)] \\ &\quad + \int_0^T [R[t, x^1(t), u^1(t)] - R[t, x^0(t), u^0(t)]] dt \\ &= \Delta_1 + \Delta_2 + \Delta_3, \end{aligned} \quad (3.12)$$

where defined that

$$\Delta_1 = G[T, x^0(T)] - G[T, x^1(T)], \quad (3.13)$$

$$\Delta_2 = \int_0^T [R(t, x^1(t), u^1(t)) - R(t, x^1(t), u^0(t))] dt, \quad (3.14)$$

$$\Delta_3 = \int_0^T [R(t, x^1(t), u^0(t)) - R(t, x^0(t), u^0(t))] dt. \quad (3.15)$$

Both conditions (3.8) (3.9) guarantee that Δ_1 and Δ_3 must be positive, and the choice of a new control (3.10) ensures the positivity of Δ_2 . These conditions assure that the new goal functional I will be smaller the the old one.

3.3 Construction of ϕ

To carry out the above iterative method the key point main and difficulty is in step (2). The condition of the functional ϕ should correspond both equations (3.8) and (3.9). That will make sure the absolute maximum of the functional R and minimum of the functional G on the old history of control $u^0(t)$ and the old trajectory $x^0(t)$. In this section, we will present the construction of ϕ to first and two order in x .

3.3.1 First Order In x

If the equation of motions of the system are linear

$$\frac{\partial x^i}{\partial t} = f^i[t, x(t), u(t)] = a_j^i[t, u(t)]x^j + b^i \quad (i = 1, 2, \dots, n), \quad (3.16)$$

and the functional $f^0[t, x(t), u(t)]$ and $F[x(T)]$ are concave with respect to $x(t)$,

$$\frac{\partial^2 f^0[t, x(t), u(t)]}{\partial x^i \partial x^i} \leq 0, \quad \frac{\partial^2 F[T, x(T)]}{\partial x^i(T) \partial x^i(T)} \leq 0. \quad (3.17)$$

then, we just need to use the first order ϕ in x . The first order means that the functional ϕ needs to satisfy both conditions (3.8) and (3.9) but do not worry about the second derivative of the functional R and G . In other words, the function ϕ just needs to satisfy the conditions that the first derivative of the functionals R and G are equal to 0. For these conditions, the functional $\phi[t, x(t)] = \Phi_i(t)x^i(t)$ should fit below conditions:

$$\begin{aligned} \frac{\partial R(t, x^0, u^0)}{\partial x} &= \frac{\partial^2 \phi(t, x^0)}{\partial x^2} f(t, x^0, u^0) + \frac{\partial \phi}{\partial x} \frac{\partial f(t, x^0, u^0)}{\partial x} - \frac{\partial f^0(t, x^0, u^0)}{\partial x} \\ &\quad + \frac{\partial}{\partial t} \frac{\partial \phi(t, x^0)}{\partial x} \\ &= \frac{\partial H(t, x^0, u^0, \Phi)}{\partial x} + \frac{\partial^2 \phi(t, x^0)}{\partial x^2} f(t, x^0, u^0) + \frac{\partial}{\partial t} \frac{\partial \phi(t, x^0)}{\partial x} \\ &= \frac{\partial H(t, x^0, u^0, \Phi)}{\partial x} + \left(\frac{\partial x}{\partial t} \frac{\partial}{\partial x} + \frac{\partial}{\partial t} \right) \frac{\partial \phi(t, x^0)}{\partial x} \\ &= \frac{\partial H(t, x^0, u^0, \Phi)}{\partial x} + \frac{d\Phi(t, x^0)}{dt} \\ &= 0, \end{aligned} \quad (3.18)$$

$$\begin{aligned} \frac{\partial G(T, x^0(T))}{\partial x(T)} &= \frac{\partial F(x^0(T))}{\partial x(T)} + \frac{\partial \phi(T, x^0(T))}{\partial x(T)} \\ &= \frac{\partial F(x^0(T))}{\partial x(T)} + \Phi(T, x^0(T)) \\ &= 0. \end{aligned} \quad (3.19)$$

Equations (3.18) and (3.19) are the equation of motion for the functional Φ :

$$\frac{d\Phi}{dt} = - \frac{\partial H[t, x^0, u^0, \Phi]}{\partial x}, \quad (3.20)$$

with boundary conditions

$$\Phi(T, x^0(T)) = - \frac{\partial F(T, x^0(T))}{\partial x(T)}, \quad (3.21)$$

and

$$\frac{dx}{dt} = \frac{\partial H[t, x^0, u^0, \Phi]}{\partial \Phi}, \quad (3.22)$$

with boundary conditions $x^0(0) = \xi$. For satisfying above conditions the easiest choice of ϕ is $\phi = \Phi[t, x(t)]x$. In the multiaraument process, the easiest choice of the functional ϕ that will also satisfy the above conditions is $\phi_i[t, x^i(t)] = \Phi_i(t)x^i(t)$.

Using the formula of the equation H (3.7), the condition becomes:

$$\dot{\Phi} = -J^T(t)\Phi(t) + \frac{\partial f^0(t, x^0, u^0)}{\partial x}, \quad (3.23)$$

where

$$J_{ij}(t) = \frac{\partial f^i(t, x^0, u^0)}{\partial x^j}, \quad (3.24)$$

and $J^T(t)$ is the transposed matrix.

3.3.2 Second Order in x

The functional ϕ can be freely chosen (3.6) but just need to satisfy both conditions (3.8) and (3.9). Therefore, we can choose the functional ϕ in the form:

$$\phi(t, x(t)) = \Phi_i(t)x^i + 0.5\sigma_{ij}(t)\Delta x^i\Delta x^j \quad (i, j = 1, 2, \dots, n). \quad (3.25)$$

where the function $\Delta(x) = x - x^0$. If we choose a suitable matrix, σ_{ij} , conditions of (3.8) and (3.9) will make the functional $\phi(t, x) \in \Pi$. It means that:

$$d^2R = \Delta x_i \frac{\partial^2 R}{\partial x^i \partial x^j} \Delta x_j, \quad dR^2 \geq 0; \quad (3.26)$$

$$d^2G = \Delta x_i(T) \frac{\partial^2 G}{\partial x^i(T) \partial x^j(T)} \Delta x_j(T), \quad -dG^2 \geq 0. \quad (3.27)$$

Because we have freedom to choose the functional ϕ , we can define that the matrix, σ_{ij} is a diagonal matrix and satisfies conditions (3.26) and (3.27). It means:

$$\begin{aligned} \frac{\partial^2 R}{\partial x^i \partial x^j} &= 0, & i \neq j, & \quad i, j = 1, 2, \dots, n; \\ \frac{\partial^2 R}{\partial x^i \partial x^i} &= \sigma_{ii}(t), & \sigma_{ii}(t) \geq 0 & \quad i = 1, 2, \dots, n; \end{aligned} \quad (3.28)$$

and

$$\begin{aligned} \frac{\partial^2 G}{\partial x^i(T) \partial x^j(T)} &= 0, & i \neq j, & \quad i, j = 1, 2, \dots, n; \\ \frac{\partial^2 G}{\partial x^i(T) \partial x^i(T)} &= \sigma_{ii}(T), & \sigma_{ii}(T) \leq 0 & \quad i = 1, 2, \dots, n. \end{aligned} \quad (3.29)$$

The matrix σ_{ij} can be determine by the linear differential (or multiaraument processes) equation (3.28) with the final condition (3.29).

3.3.3 Algorithm

In previous section, we have already introduced Krotov method. In this section, we will summarize the algorithm step by step.

STEP 1: Freely choose a history of control process, named $u^0(t)$.

STEP 2: Using the equation (3.1) and initial conditions $x(0) = \xi$ finds the trajectory $x^0(t)$.

STEP 3: By equations (3.23) with the final condition (3.21), a vector-function $\Phi(t)$ is found.

STEP 4: Using conditions (3.28) and (3.29), the matrix σ_{ij} is defined.

STEP 5: For this function ϕ , the control \tilde{u} is found according to equation (3.10).

STEP 6: The new trajectory $x^i(t)$ and the new history of control $u^1(t)$ is found by (3.1).

STEP 7: Repeat STEP 2 to STEP 6, until the optimal value is found.

3.4 Discrete time interval system

This Krotov method not only can deal with the continuous in time problems, but also can handle discrete time interval problems. Consider a discrete in time problem:

$$x(t+1) = f(t, x, u), \quad t = 1, 2, \dots, T-1; \quad x(0) = \xi; \quad u \in U; \quad (3.30)$$

$$I[x(t), u(t)] = \sum_{t=0}^{T-1} f^0(t, x(t), u(t)) + F(x(T)) \rightarrow \min. \quad (3.31)$$

In the discrete in time system the optimal control method is similar to the continuous in time system. We may define a functional $L[t, x(t), u(t), \phi]$ satisfying the result of Eq.(3.6). To satisfy the condition, we can define the functional form as:

$$R[t, x(t), u(t)] = \phi[t+1, x(t+1)] - \phi[t, x(t)] - f^0(t, x(t), u(t)), \quad (3.32)$$

$$G[T, x(T)] = F[T, x(T)] + \phi(T, x(T)), \quad (3.33)$$

$$L[t, x(t), u(t), \phi] = -\left(\sum_0^{T-1} R[t, x(t), u(t)]\right) - \phi(0, x(0)) + G[t, x(T)]. \quad (3.34)$$

It is easy to show that the functional ϕ can be an arbitrary functional. Similar to that in the continuous systems, but satisfy conditions (3.8) and (3.9). we may choose the functional, ϕ , to have the same form as that for the continuous systems, Eq.(3.25). Although, a discrete problem in time problem may not be practical, it is useful to design and understand its algorithm. We will show a discrete example in the section 3.5.

3.5 Examples

3.5.1 Discrete variant

This problem comes from (A.I. Propoi [7]).

The goal function:

$$I = -x^{(2)}(2) \rightarrow \min$$

where $x^{(2)}(2)$ means the value of the second trajectory at 2 second, and the equations of motion:

$$\begin{aligned} x^{(1)}(t+1) &= x^{(1)}(t) + 2u(t), \\ x^{(2)}(t+1) &= -(x^{(1)}(t))^2 + x^{(2)}(t) + u^2(t), \\ t = 0, 1 \quad x^{(1)}(0) &= 3, \quad x^{(2)}(0) = 0, \quad -5 \leq u(t) \leq 5. \end{aligned}$$

Because the equations of motion are not linear, the function of $\phi(t, x)$ should take the form:

$$\phi(t, x) = \Phi_1(t)x^{(1)} + \Phi_2(t)x^{(2)} + \sigma_{11} \frac{(x^{(1)} - x^{(1)0}(t))^2}{2} + \sigma_{22} \frac{(x^{(2)} - x^{(2)0}(t))^2}{2}; \quad (3.35)$$

where $x^{(i)0}$ means each current trajectory. The function of ϕ just needs to satisfy conditions (3.28) and (3.29), so we can take $\sigma_{22} = 0$ and $\sigma_{11} = \sigma$. Then equation (3.35) becomes to :

$$\phi(t, x) = \Phi_1(t)x^{(1)} + \Phi_2(t)x^{(2)} + \sigma \frac{(x^{(1)} - x^{(1)0}(t))^2}{2}. \quad (3.36)$$

Therefore, the functional R and G take the form:

$$\begin{aligned}
R(t, x, u) &= \Phi_1(t+1)(x^{(1)}(t+1)) + \Phi_2(t+1)(x^{(2)}(t+1)) \\
&\quad + 0.5\sigma(x^{(1)}(t+1) - x^{(1)0}(t+1))^2 - \Phi_1(t)(x^{(1)}(t)) \\
&\quad - \Phi_2(t)(x^{(2)}(t)) - 0.5\sigma(x^{(1)}(t) - x^{(1)0}(t))^2 \\
&= \Phi_1(t+1)(x^{(1)}(t) + 2u(t)) \\
&\quad + \Phi_2(t+1)(-(x^{(1)})^2(t) + x^{(2)}(t) + u^2(t)) \\
&\quad + 0.5\sigma(t+1)(x^{(1)} + 2u - x^{(1)0})^2 - \Phi_1(t)x^{(1)}(t) \\
&\quad - \Phi_2(t)x^{(2)} - 0.5\sigma(2)(x^{(1)} - x^{(1)0}(t))^2, \tag{3.37}
\end{aligned}$$

$$\begin{aligned}
G(x(T)) &= -x^{(2)}(T) + \Phi_1(2)x^{(1)}(2) + \Phi_2(2)x^{(2)}(2) \\
&\quad + 0.5\sigma(2)(x^{(1)}(2) - x^{(1)0}(2))^2. \tag{3.38}
\end{aligned}$$

Using conditions (3.28) and 3.29), we can get equations Φ and σ :

$$\begin{aligned}
\Phi_1(t) &= \Phi_1(t+1) - 2x^{(1)0}(t)\Phi_2(t+1), & \Phi_1(2) &= 0; \\
\Phi_2(t) &= \Phi_2(t+1), & \Phi_2(2) &= 1; \\
\sigma(t) &= -2\Phi_2(t+1) + \sigma(t+1) - \delta, & \sigma(2) &= \alpha. \tag{3.39}
\end{aligned}$$

Choose the simplest the history of control $u^0(t)$: $u(0) = u(1) = 0$. Define $\delta = 0$ and $\alpha = -1$ to determine the matrix of σ . The results are shown in Table 3.1. It is clear from Table 3.1 that when the iteration runs to 15, we can get the minimum value of the goal functional I . Also, we can know all of the iteration processes of the optimal control.

3.5.2 The Continuous in Time System With One Equation of Motion

Consider the problem in [6]. The equation of motion is

$$\dot{x} = u, \quad |u| \leq 1, \quad x(0) = x(T) = 0; \tag{3.40}$$

and the goal functional

$$I = \int_0^T (u^2 - x^2)dt + \frac{1}{2}bx^2(T) \rightarrow \min, \tag{3.41}$$

| No. | $u(1)$ | $u(2)$ | $x^{(1)}(1)$ | $x^{(1)}(2)$ | $x^{(2)}(1)$ | $x^{(2)}(2)$ | $\Phi_1(1)$ | $\Phi_2(1)$ | I |
|-----|---------|--------|--------------|--------------|--------------|--------------|-------------|-------------|----------|
| 1 | 0 | 0 | 3.0000 | 3.0000 | -9.0000 | -18.0000 | -6.0000 | 1.0000 | 18.0000 |
| 2 | -1.2000 | 2.4000 | 0.6000 | 5.4000 | -7.5600 | -2.1600 | -1.2000 | 1.0000 | 2.1600 |
| 3 | -1.6800 | 5.0000 | -0.3600 | 9.6400 | -6.1776 | 18.6928 | 0.7200 | 1.0000 | -18.6928 |
| 4 | -1.8720 | 5.0000 | -0.7440 | 9.2560 | -5.4956 | 18.9508 | 1.4880 | 1.0000 | -18.9508 |
| 5 | -1.9488 | 5.0000 | -0.8976 | 9.1024 | -5.2022 | 18.9921 | 1.7952 | 1.0000 | -18.9921 |
| 6 | -1.9795 | 5.0000 | -0.9590 | 9.0410 | -5.0815 | 18.9987 | 1.9181 | 1.0000 | -18.9987 |
| 7 | -1.9918 | 5.0000 | -0.9836 | 9.0164 | -5.0327 | 18.9998 | 1.9672 | 1.0000 | -18.9998 |
| 8 | -1.9967 | 5.0000 | -0.9934 | 9.0066 | -5.0131 | 19.0000 | 1.9869 | 1.0000 | -19.0000 |
| 9 | -1.9987 | 5.0000 | -0.9974 | 9.0026 | -5.0052 | 19.0000 | 1.9948 | 1.0000 | -19.0000 |
| 10 | -1.9995 | 5.0000 | -0.9990 | 9.0010 | -5.0021 | 19.0000 | 1.9979 | 1.0000 | -19.0000 |
| 11 | -1.9998 | 5.0000 | -0.9996 | 9.0004 | -5.0008 | 19.0000 | 1.9992 | 1.0000 | -19.0000 |
| 12 | -1.9999 | 5.0000 | -0.9998 | 9.0002 | -5.0003 | 19.0000 | 1.9997 | 1.0000 | -19.0000 |
| 13 | -2.0000 | 5.0000 | -0.9999 | 9.0001 | -5.0001 | 19.0000 | 1.9999 | 1.0000 | -19.0000 |
| 14 | -2.0000 | 5.0000 | -1.0000 | 9.0000 | -5.0001 | 19.0000 | 1.9999 | 1.0000 | -19.0000 |
| 15 | -2.0000 | 5.0000 | -1.0000 | 9.0000 | -5.0000 | 19.0000 | 2.0000 | 1.0000 | -19.0000 |
| 16 | -2.0000 | 5.0000 | -1.0000 | 9.0000 | -5.0000 | 19.0000 | 2.0000 | 1.0000 | -19.0000 |

Table 3.1: Evolution of functional with the iteration numbers. The iteration number is denoted in "No." column. .

where $b > 0$.

Now, we solve the problem with the following parameters: $b = 10$, $T = 4$ by using Krotov method. Using Eq.(3.3) and Eq.(3.4) and the form of ϕ (3.25), the functionals R and G can be written as:

$$R = \dot{\Phi}(t)x(t) + \frac{1}{2}\dot{\sigma}(t)(\Delta x(t))^2 + \Phi(t)u(t) + \sigma\Delta x(t)(u(t) - u^0(t)) - u^2(t) + x^2(t), \quad (3.42)$$

$$G = \Phi(T)x(T) + \frac{1}{2}\sigma(T)(\Delta x(T))^2 + \frac{1}{2}bx^2(T). \quad (3.43)$$

Since $R_{xx} = \frac{1}{2}\dot{\sigma}(t)+1$ and $G_{xx} = \sigma(T)+b$, we choose that $\sigma(\dot{t}) = 0$ and $\sigma(T) = -b-4$. Performing the algorithm, we obtain the result shown in Fig.(3.1) We just show the result of the 1st, 3rd, 5th and 7th iterations in Fig.(3.1). The 8th and 9th iterations are the same as the 7th. We use the 4th order Runge Kutta method with the segment of integration partitioned into 200 pieces. Also, this result is consisted with the known solution of this problem. The solution is

$$x(t) = \begin{cases} \pm t & t \leq \tau_1, \\ \pm k \cos(t - T/2) & \tau_1 \leq t \leq \tau_2. \\ \pm T \mp t & \tau_2 \leq t, \end{cases}$$

where T means the final time, and τ_1 , τ_2 and k are chosen according to smoothness conditions, that is, $\dot{x} = \pm 1$ for $t = \tau_1$, $\dot{x} = \mp 1$ for $t = \tau_2$, $\pm t = \pm k \cos(t - T/2)$ at $t = \tau_1$ and $\pm k \cos(t - T/2) = \pm T \mp t$ at $t = \tau_2$. If we plot this solution and the final iteration result on the same graph. It will overlaps with the solid-line curve in Fig.(3.1). This demonstrates the validity and usefulness of the Krotov method. We will apply this optimal method to investigate quantum gate operations in later chapters.

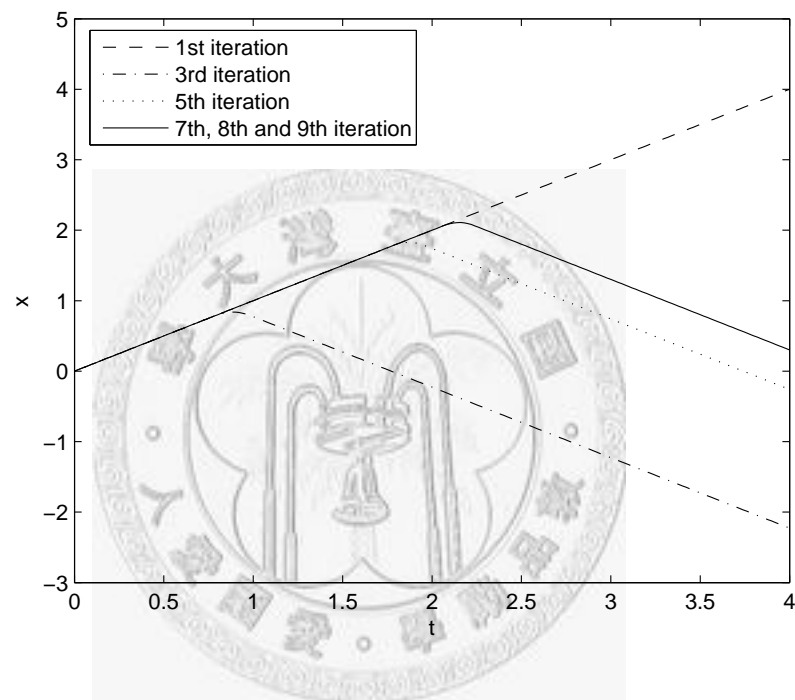


Figure 3.1: Optimal evolution of x for different numbers of iterations

Chapter 4

Quantum system with Environment

4.1 Master Equation

4.1.1 Density Matrix

For a closed quantum system, the physical object obeys Schrödinger equation,

$$\frac{\partial}{\partial t}|\psi_i \rangle = -\frac{i}{\hbar}H|\psi_i \rangle, \quad (4.1)$$

where H is the total Hamiltonian. The density matrix can be defined as,

$\rho = \sum_i P_i |\psi_i \rangle \langle \psi_i|$, where the coefficients, P_i , are non-negative and time independent. Using Schrödinger equation Eq.(4.1), we can get the equation of motion of the density matrix $\dot{\rho}$,

$$\begin{aligned} \dot{\rho} &= \sum_i P_i (|\dot{\psi}_i \rangle \langle \psi_i| + |\psi_i \rangle \langle \dot{\psi}_i|) \\ &= \sum_i P_i \left(-\frac{i}{\hbar} H |\psi_i \rangle \langle \psi_i| + \frac{i}{\hbar} |\psi_i \rangle \langle \psi_i| H \right) \\ &= -\frac{i}{\hbar} \left(H \sum_i P_i |\psi_i \rangle \langle \psi_i| - \sum_i P_i |\psi_i \rangle \langle \psi_i| H \right) \\ &= -\frac{i}{\hbar} (H\rho - \rho H) \\ &= -\frac{i}{\hbar} [H, \rho], \end{aligned} \quad (4.2)$$

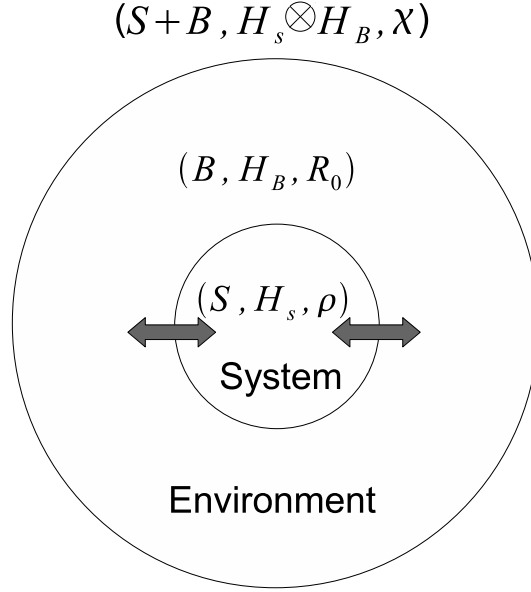


Figure 4.1: Schematic picture of an open system

Equation (4.2) is called Liouville-Von Neumann equation of motion for the density matrix. Note that Liouville equation, Eq. (4.2), can only be used in a closed quantum system. Hence, it is not valid for the subsystem of a composite system whose subsystems have interaction with one another. The equation can only describe the whole system including the subsystem in which we are interested and the rest of the system. In the next section, we will discuss how to write down the equation of motion for the subsystem in which we are interested.

4.1.2 Derivation of Master Equation

Because Eq.(4.2) can only be used in closed system, when we solve a composite system, we can divide the system into two part. A schematic picture is shown in Fig.4.1 One part is the subsystem in which we are interested, the other part is a bath. The Hamiltonian of the subsystem is time-dependent, $H_S(t)$, and the bath is the rest system with Hamiltonian, H_B . Also, consider that the subsystem and bath are couple to each other, and the interaction Hamiltonian of the coupling term is

denoted as H_{SB} . Hence, the total Hamiltonian can be written as,

$$H(t) = H_S(t) \otimes I_B + I_S \otimes H_B + H_{SB}, \quad (4.3)$$

and the Hilbert space of the total system is defined by a tensor product,

$$\mathcal{H} = H_S \otimes H_B. \quad (4.4)$$

Define the total density matrix (subsystem and bath) as $\chi(t)$ obeying Liouville-Von Neumann equation (4.2),

$$\dot{\chi}(t) = -\frac{i}{\hbar}[H(t), \chi(t)], \quad (4.5)$$

where $H(t)$ is given by Eq. (4.3). Usually we assume that the interaction Hamiltonian of the subsystem and bath is very weak compared with the rest of the Hamiltonian. Therefore, we may use the interaction picture to fix the dominant term, the subsystem and bath, $H_S + H_B$. Define

$$\begin{aligned} \tilde{\chi}(t) &= e^{\frac{i}{\hbar}(H_S+H_B)t} \chi(t) e^{-\frac{i}{\hbar}(H_S+H_B)t}, \\ \chi(t) &= e^{-\frac{i}{\hbar}(H_S+H_B)t} \tilde{\chi}(t) e^{\frac{i}{\hbar}(H_S+H_B)t}, \end{aligned} \quad (4.6)$$

and take a deviative of Eq.(4.6) respect with time, we obtain

$$\begin{aligned} \dot{\chi}(t) &= -\frac{i}{\hbar}(H_S + H_B) e^{-\frac{i}{\hbar}(H_S+H_B)t} \tilde{\chi}(t) e^{\frac{i}{\hbar}(H_S+H_B)t} \\ &\quad + e^{-\frac{i}{\hbar}(H_S+H_B)t} \dot{\tilde{\chi}}(t) e^{\frac{i}{\hbar}(H_S+H_B)t} \\ &\quad + \frac{i}{\hbar} e^{-\frac{i}{\hbar}(H_S+H_B)t} \tilde{\chi}(t) (H_S + H_B) e^{\frac{i}{\hbar}(H_S+H_B)t}. \end{aligned} \quad (4.7)$$

Using Eq.(4.5), we obtain

$$\begin{aligned} \dot{\chi}(t) &= -\frac{i}{\hbar}[H_S + H_B + H_{SB}, \chi(t)] \\ &= -\frac{i}{\hbar}(H_S + H_B + H_{SB}) e^{-\frac{i}{\hbar}(H_S+H_B)t} \tilde{\chi}(t) e^{\frac{i}{\hbar}(H_S+H_B)t} \\ &\quad + \frac{i}{\hbar} e^{-\frac{i}{\hbar}(H_S+H_B)t} \tilde{\chi}(t) e^{\frac{i}{\hbar}(H_S+H_B)t} (H_S + H_B + H_{SB}). \end{aligned} \quad (4.8)$$

Comparing with Eq.(4.7) and Eq.(4.8), we obtain

$$\begin{aligned} &e^{-\frac{i}{\hbar}(H_S+H_B)t} \dot{\tilde{\chi}}(t) e^{\frac{i}{\hbar}(H_S+H_B)t} \\ &= -\frac{i}{\hbar} H_{SB} e^{-\frac{i}{\hbar}(H_S+H_B)t} \tilde{\chi}(t) e^{\frac{i}{\hbar}(H_S+H_B)t} \\ &\quad + \frac{i}{\hbar} e^{-\frac{i}{\hbar}(H_S+H_B)t} \tilde{\chi}(t) e^{\frac{i}{\hbar}(H_S+H_B)t} H_{SB}. \end{aligned} \quad (4.9)$$

Defining

$$\tilde{H}_{SB}(t) = e^{\frac{i}{\hbar}(H_S+H_B)t} H_{SB} e^{-\frac{i}{\hbar}(H_S+H_B)t}, \quad (4.10)$$

and substituting Eq.(4.10) into Eq.(4.9), we obtain

$$\begin{aligned} \dot{\tilde{\chi}}(t) &= -\frac{i}{\hbar} e^{\frac{i}{\hbar}(H_S+H_B)t} H_{SB} e^{-\frac{i}{\hbar}(H_S+H_B)t} \tilde{\chi}(t) + \frac{i}{\hbar} \tilde{\chi}(t) e^{\frac{i}{\hbar}(H_S+H_B)t} H_{SB} e^{-\frac{i}{\hbar}(H_S+H_B)t} \\ &= -\frac{i}{\hbar} [\tilde{H}, \tilde{\chi}(t)]. \end{aligned} \quad (4.11)$$

We may then obtain the integral form of Eq.(4.11) as

$$\tilde{\chi}(t) = \tilde{\chi}(0) + \frac{i}{\hbar} \int_0^t \frac{i}{\hbar} [\tilde{H}_{SB}(t'), \tilde{\chi}(t')] dt'. \quad (4.12)$$

Substituting Eq.(4.12) back into Eq.(4.11), we can get

$$\begin{aligned} \dot{\tilde{\chi}}(t) &= -\frac{i}{\hbar} [\tilde{H}_{SB}(t), \tilde{\chi}(0) + \frac{i}{\hbar} \int_0^t \frac{i}{\hbar} [\tilde{H}_{SB}(t'), \tilde{\chi}(t')] dt'] \\ &= -\frac{i}{\hbar} [\tilde{H}_{SB}(t), \tilde{\chi}(0)] - \frac{1}{\hbar^2} \int_0^t [\tilde{H}_{SB}(t), [\tilde{H}_{SB}(t'), \tilde{\chi}(t')]]. \end{aligned} \quad (4.13)$$

However, we are just interested in the evolution of the subsystem. Hence, we can define the density matrix of the subsystem as ρ satisfying that

$$\rho(t) = Tr_{bath}[\chi(t)] = Tr_B[\chi(t)]. \quad (4.14)$$

If we take the trace of the full density matrix over the bath, in the interaction picture, we obtain

$$\begin{aligned} Tr_B[\tilde{\chi}(t)] &= Tr_B[e^{\frac{i}{\hbar}(H_S+H_B)t} \chi(t) e^{-\frac{i}{\hbar}(H_S+H_B)t}] \\ &= e^{\frac{i}{\hbar}H_S t} Tr_B[e^{\frac{i}{\hbar}H_B t} \chi(t) e^{-\frac{i}{\hbar}H_B t}] e^{-\frac{i}{\hbar}H_S t} \\ &= e^{\frac{i}{\hbar}H_S t} \left[\sum_i \langle \phi_i^B | e^{\frac{i}{\hbar}H_B t} \chi(t) e^{-\frac{i}{\hbar}H_B t} | \phi_i^B \rangle \right] e^{-\frac{i}{\hbar}H_S t} \\ &= e^{\frac{i}{\hbar}H_S t} \left[\sum_i \langle \phi_i^B | e^{\frac{i}{\hbar}E_i^B t} \chi(t) e^{-\frac{i}{\hbar}E_i^B t} | \phi_i^B \rangle \right] e^{-\frac{i}{\hbar}H_S t} \\ &= e^{\frac{i}{\hbar}H_S t} \left[\sum_i \langle \phi_i^B | \chi(t) | \phi_i^B \rangle \right] e^{-\frac{i}{\hbar}H_S t} \\ &= e^{\frac{i}{\hbar}H_S t} Tr_B[\chi(t)] e^{-\frac{i}{\hbar}H_S t} \\ &= e^{\frac{i}{\hbar}H_S t} \rho e^{-\frac{i}{\hbar}H_S t} \\ &= \tilde{\rho}(t), \end{aligned} \quad (4.15)$$

where E_i^B and $|\phi_i^B\rangle$ correspond to the eigenvalue and eigenstate of H_B . Thus, in the interaction picture, the density matrix of the subsystem can be shown to be

$$\tilde{\rho}(t) = e^{\frac{i}{\hbar}H_S t} \rho e^{-\frac{i}{\hbar}H_S t}. \quad (4.16)$$

It means that the transformation between ρ and $\tilde{\rho}$ only depends on the Hamiltonian of the subsystem H_S . Using Eq.(4.13) and Eq.(4.15), we obtain

$$\begin{aligned} \dot{\tilde{\rho}}(t) &= \frac{\partial}{\partial t} Tr_B[\tilde{\chi}(t)] = Tr_B[\dot{\tilde{\chi}}(t)] \\ &= -\frac{i}{\hbar} [\tilde{H}_{SB}(t), \tilde{\chi}(0)] - \frac{1}{\hbar^2} \int_0^t [\tilde{H}_{SB}(t), [\tilde{H}_{SB}(t'), \tilde{\chi}(t')]] dt'. \end{aligned} \quad (4.17)$$

Usually, Eq.(4.17) is difficult to solve in general case. In the next two sections, we will introduce two approximations to solve Eq.(4.17).

4.1.3 Born Approximation

We assume that there is no interaction and correlation between the subsystem and bath, before $t = 0$. Hence, $\tilde{\chi}(0) = \chi(0)$ and

$$\chi(0) = \rho(0) \otimes R_0, \quad (4.18)$$

where R_0 is an initial density matrix of the bath. If the bath is very big and the coupling interaction H_{SB} is very weak, we can assume that the bath as a reservoir. Hence, we can assume that when $t > 0$ the density matrix of the bath is the same as initial density matrix,

$$\tilde{\chi}(t) = \tilde{\rho}(t) \otimes R_0. \quad (4.19)$$

Therefore, Born approximation has two points:

- (1) We don't care about what happen before we detect or operate the subsystem.
- (2) The density matrix of the bath is independent of time.

We usually assume that the density matrix of the bath stays in thermal equilibrium,

$$R_0 = \frac{e^{-\beta H_B}}{Tr e^{-\beta(H_B)}}. \quad (4.20)$$

Substituting Eq.(4.18) and Eq.(4.19) into Eq.(4.17), we have

$$\begin{aligned}\dot{\rho}(t) &= -\frac{i}{\hbar}Tr_B[\tilde{H}_{SB}(t), \rho(0) \otimes R_0] \\ &\quad -\frac{1}{\hbar^2} \int_0^t Tr_B[\tilde{H}_{SB}(t), [\tilde{H}_{SB}(t'), \tilde{\rho}(t') \otimes R_0]]dt'.\end{aligned}\quad (4.21)$$

We thus find in the Born approximation the equation of motion or master equation of the $\tilde{\rho}$, Eq.(4.21). However, usually Eq.(4.21) is very complicated, because the term $\tilde{\rho}(t')$ is influenced by not only present states but also the past evolution of states. We will use one more assumption, Markovian approximation, to simplify Eq.(4.21). In the next section, we will introduce the Markovian approximation.

4.1.4 Markovian Approximation

The most general form of coupling interaction, H_{SB} , can be defined as

$$H_{SB} = \sum_j S_j \otimes B_j, \quad (4.22)$$

where S_j are the system operators and B_j are the bath operators. Inserting Eq.(4.22) into Eq.(4.21),

$$\begin{aligned}\dot{\rho}(t) &= -\frac{i}{\hbar} \sum_j Tr_B[\tilde{S}_j(t) \otimes \tilde{B}_j(t), \tilde{\rho}(0) \otimes R_0] \\ &\quad -\frac{1}{\hbar^2} \int_0^t \sum_{j,k} Tr_B[S_j \otimes B_j, [S_k \otimes B_k, \tilde{\rho}(t') \otimes R_0]]dt'.\end{aligned}\quad (4.23)$$

If we consider a thermal bath, then the bath operator average in the thermal equilibrium state R_0 , Eq.(4.20), vanishes:

$$Tr[\tilde{B}_k(t)R_0] = 0. \quad (4.24)$$

According to Eq.(4.24), the first term of Eq.(4.21) vanishes. Also, in the second term, we will obtain

$$C_{jk}(t-t') \equiv Tr_B[\tilde{B}_j(t)\tilde{B}_k(t')R_0], \quad (4.25)$$

named the bath correlation functions. In the Markovian approximation, we assume that the bath correlation time is much smaller than typical system response time.

In mathematics, this means that the both correlation function C_{jk} isn't zero only at $t = t'$. Hence,

$$C_{jk} \propto \delta(t - t'), \quad (4.26)$$

in this condition, the $\tilde{\rho}(t')$ can be replaced by $\tilde{\rho}(t)$, in the second term of Eq.(4.21). Therefore, the density matrix of the subsystem, $\tilde{\rho}$ only depends on its present state. Also, because of the property of the bath correlation functions, we can change the time range of the Eq.(4.23) to $t = \infty$. With the above assumptions, Eq.(4.21) can be rewritten to,

$$\dot{\rho}(t) = -\frac{1}{\hbar^2} \int_0^\infty Tr_B[\tilde{H}_{SB}(t), [\tilde{H}_{SB}(t - t'), \tilde{\rho}(t) \otimes R_0]] dt', \quad (4.27)$$

called the Born-Markov master equation in the interaction picture. Using following relation,

$$\begin{aligned} \tilde{\rho}(t) &\equiv e^{\frac{i}{\hbar}H_S t} \rho e^{-\frac{i}{\hbar}H_S t} \\ \Rightarrow \frac{d}{dt} \tilde{\rho}(t) &= \frac{i}{\hbar} [H_S, \tilde{\rho}(t)] + e^{\frac{i}{\hbar}H_S t} \frac{d}{dt} \rho e^{-\frac{i}{\hbar}H_S t} \\ \Rightarrow \frac{d}{dt} \rho(t) &= -\frac{i}{\hbar} [H_S, \rho(t)] + e^{\frac{i}{\hbar}H_S t} \frac{d}{dt} \tilde{\rho} e^{-\frac{i}{\hbar}H_S t}, \end{aligned} \quad (4.28)$$

we can get the Born-Markov master equation in the Schrödinger picture, and the form is

$$\dot{\rho}(t) = -\frac{i}{\hbar} [H_S, \rho(t)] - \frac{1}{\hbar^2} \int_0^\infty Tr_B[\tilde{H}_{SB}(t), [\tilde{H}_{SB}(t - t'), \tilde{\rho}(t) \otimes R_0]] dt'. \quad (4.29)$$

We use the general form of the interaction between the subsystem and environment

$$H_{SB} = \hbar \sum_i s_i \Gamma_i; \quad (4.30)$$

where the s_i are operators in the subsystem and Γ_i in the environment. Then, in the interaction picture we can get

$$\tilde{H}_{SB}(t) = \hbar \sum_i \tilde{s}_i(t) \tilde{\Gamma}_i(t). \quad (4.31)$$

Insert Eq.(4.31) into Eq.(4.27), we can get

$$\dot{\tilde{\rho}} = - \sum_{i,j} \int_0^\infty Tr_B[\tilde{s}_i(t)\tilde{\Gamma}_i(t), [\tilde{s}_j(t')\tilde{\Gamma}_j(t'), \tilde{\rho}(t') \otimes R_0]] dt', \quad (4.32)$$

$$\begin{aligned} &= - \sum_{i,j} \int_0^\infty ((\tilde{s}_i(t)\tilde{s}_j(t')\tilde{\rho}(t') - \tilde{s}_j(t')\tilde{\rho}(t')\tilde{s}_i(t)) \langle \tilde{\Gamma}_i(t)\tilde{\Gamma}_j(t') \rangle_R \\ &\quad + [\tilde{\rho}(t')\tilde{s}_j(t')\tilde{s}_i(t) - \tilde{s}_i\tilde{\rho}(t')\tilde{s}_j(t')] \langle \tilde{\Gamma}_j(t')\tilde{\Gamma}_i(t) \rangle_R) dt', \end{aligned} \quad (4.33)$$

where we define that

$$\langle \tilde{\Gamma}_i(t)\tilde{\Gamma}_j(t') \rangle_R = Tr[R_0\tilde{\Gamma}_i(t)\tilde{\Gamma}_j(t')], \quad (4.34)$$

$$\langle \tilde{\Gamma}_j(t')\tilde{\Gamma}_i(t) \rangle_R = Tr[R_0\tilde{\Gamma}_j(t')\tilde{\Gamma}_i(t)]. \quad (4.35)$$

Also we can get the specific form in the Schrödinger picture.

4.2 Master Equation for a Two-Level System

4.2.1 Thermal Equilibrium

We consider a two level system ($|0\rangle$ and $|1\rangle$ with $E_0 < E_1$) with Hamiltonian:

$$H_S = \frac{1}{2}\hbar w_A \sigma_z, \quad (4.36)$$

$$H_R = \sum_{k,\lambda} \hbar w_k \gamma_{k,\lambda}^\dagger \gamma_{k,\lambda}, \quad (4.37)$$

$$H_{SR} = \sum_{k,\lambda} \hbar(\kappa_{k,\lambda}^* \gamma_{k,\lambda}^\dagger \sigma_- + \kappa_{k,\lambda} \gamma_{k,\lambda} \sigma_+), \quad (4.38)$$

with

$$\kappa_{k,\lambda} = -ie^{ik\cdot\gamma_A} \sqrt{\frac{w_k}{2\hbar\epsilon_0 V}} \hat{e}_{k,\lambda} \cdot d_{21}, \quad (4.39)$$

where H_S is Hamiltonian of the system, H_R Hamiltonian of the reservoir and H_{SR} Hamiltonian of the interaction between system and reservoir. The summation extends over reservoir oscillators with wavevectors k and polarization states λ , and corresponding frequencies w_k and unit polarization vector $\hat{e}_{k,\lambda}$. The system is positioned at γ_A and V is the quantization volume. Comparing with Eq.(4.30), we can

get the relation

$$s_1 = \sigma_-, \quad s_2 = \sigma_+, \quad (4.40)$$

$$\Gamma_1 = \Gamma^\dagger = \sum_{k,\lambda} \kappa_{k,\lambda}^* \gamma_{k,\lambda}^\dagger, \quad \Gamma_2 = \Gamma = \sum_{k,\lambda} \kappa_{k,\lambda} \gamma_{k,\lambda}. \quad (4.41)$$

In the interaction picture,

$$\tilde{s}_1(t) = e^{i(w_A \sigma_z/2)t} \sigma_- e^{-i(w_A \sigma_z/2)t} = \sigma_- e^{-i w_A t}, \quad (4.42)$$

$$\tilde{s}_2(t) = e^{i(w_A \sigma_z/2)t} \sigma_+ e^{-i(w_A \sigma_z/2)t} = \sigma_+ e^{i w_A t}, \quad (4.43)$$

$$\tilde{\Gamma}_1(t) = \tilde{\Gamma}^\dagger(t) = \sum_{k,\lambda} \kappa_{k,\lambda}^* \gamma_{k,\lambda}^\dagger e^{i w_k t}, \quad (4.44)$$

$$\tilde{\Gamma}_2(t) = \tilde{\Gamma}(t) = \sum_{k,\lambda} \kappa_{k,\lambda} \gamma_{k,\lambda} e^{-i w_k t}, \quad (4.45)$$

Now, since the summation in Eq.(4.33) runs over $i = 1, 2$ and $j = 1, 2$. Also, substituting the above equations into Eq.(4.33), we obtain

$$\begin{aligned} \dot{\rho} = & - \int_0^\infty ([\sigma_- \sigma_- \tilde{\rho}(t') - \sigma_- \tilde{\rho}(t') \sigma_-] e^{-i w_A(t+t')} \langle \tilde{\Gamma}^\dagger(t) \tilde{\Gamma}^\dagger(t') \rangle_R + h.c. \\ & + [\sigma_+ \sigma_+ \tilde{\rho}(t') - \sigma_+ \tilde{\rho}(t') \sigma_+] e^{i w_A(t+t')} \langle \tilde{\Gamma}(t) \tilde{\Gamma}(t') \rangle_R + h.c. \\ & + [\sigma_- \sigma_+ \tilde{\rho}(t') - \sigma_+ \tilde{\rho}(t') \sigma_-] e^{-i w_A(t-t')} \langle \tilde{\Gamma}^\dagger(t) \tilde{\Gamma}(t') \rangle_R + h.c. \\ & + [\sigma_+ \sigma_- \tilde{\rho}(t') - \sigma_- \tilde{\rho}(t') \sigma_+] e^{i w_A(t-t')} \langle \tilde{\Gamma}(t) \tilde{\Gamma}^\dagger(t') \rangle_R + h.c.) dt'. \end{aligned} \quad (4.46)$$

Now, we take the reservoir to be in thermal equilibrium at temperature T , then

$$R_0 = \prod_j e^{-\hbar w_k \gamma_{k,\lambda}^\dagger \gamma_{k,\lambda} / k_B T} (1 - e^{-\hbar w_k / k_B T}), \quad (4.47)$$

where k_B is Boltzmann's constant. Hence, we can get

$$\langle \tilde{\Gamma}^\dagger(t) \tilde{\Gamma}^\dagger(t') \rangle_R = 0, \quad (4.48)$$

$$\langle \tilde{\Gamma}(t) \tilde{\Gamma}(t') \rangle_R = 0, \quad (4.49)$$

$$\langle \tilde{\Gamma}^\dagger(t) \tilde{\Gamma}(t') \rangle_R = \sum_j |\kappa_j|^2 e^{i w_j(t-t')} \bar{n}(w_j, T), \quad (4.50)$$

$$\langle \tilde{\Gamma}(t) \tilde{\Gamma}^\dagger(t') \rangle_R = \sum_j |\kappa_j|^2 e^{-i w_j(t-t')} [\bar{n}(w_j, T) + 1], \quad (4.51)$$

with

$$\bar{n}(w_j, T) = Tr_R(R_0 \gamma_j^\dagger \gamma_j) = \frac{e^{-\hbar w_j / k_B T}}{1 - e^{-\hbar w_j / k_B T}}, \quad (4.52)$$

where $\bar{n}(w_j, T)$ is the mean number for an oscillator with frequency w_j in thermal equilibrium at temperature T . Therefore, by using these relations Eqs.(4.48) ~ (4.51) and making a change of variable $\tau = t - t'$, Eq.(4.46) becomes

$$\begin{aligned} \dot{\rho} = & - \int_0^\infty ([\sigma_- \sigma_+ \tilde{\rho}(t - \tau) - \sigma_+ \tilde{\rho}(t - \tau) \sigma_-] e^{i w_A \tau} \langle \tilde{\Gamma}^\dagger(t) \tilde{\Gamma}(t - \tau) \rangle_R \\ & + [\sigma_+ \sigma_- \tilde{\rho}(t - \tau) - \sigma_- \tilde{\rho}(t - \tau) \sigma_+] e^{i w_A \tau} \langle \tilde{\Gamma}(t) \tilde{\Gamma}^\dagger(t - \tau) \rangle_R) d\tau. \end{aligned} \quad (4.53)$$

Because, in the Markovian approximation, the τ integration in Eq.(4.53) are much shorter than the time scale for the evolution of $\tilde{\rho}$, we can replace $\tilde{\rho}(t - \tau)$ by $\tilde{\rho}(t)$ and get

$$\begin{aligned} \dot{\rho} = & [\frac{\gamma}{2}(\bar{n} + 1) + i(\Delta' + \Delta)](\sigma_- \tilde{\rho} \sigma_+ - \sigma_+ \sigma_- \tilde{\rho}) \\ & + [\frac{\gamma}{2}\bar{n} + i\Delta'(\sigma_+ \tilde{\rho} \sigma_- - \tilde{\rho} \sigma_- \sigma_+)], \end{aligned} \quad (4.54)$$

where

$$\gamma = 2\pi \sum_\lambda \int g(k) |\kappa(k, \lambda)|^2 \delta(kc - w_A) d^3k, \quad (4.55)$$

$$\Delta = \sum_\lambda P \int \frac{g(k) |\kappa(k, \lambda)|^2}{w_A - kc} d^3k, \quad (4.56)$$

$$\Delta' = \sum_\lambda P \int \frac{g(k) |\kappa(k, \lambda)|^2}{w_A - kc} \bar{n}(kc, T) d^3k. \quad (4.57)$$

Using the following relations

$$\sigma_+ \sigma_- = \frac{1}{2}(1 + \sigma_z), \quad (4.58)$$

$$\sigma_- \sigma_+ = \frac{1}{2}(1 - \sigma_z), \quad (4.59)$$

we obtain

$$\begin{aligned} \dot{\rho} = & -i\frac{1}{2}(2\Delta' + \Delta)[\sigma_z, \tilde{\rho}] + \frac{\gamma}{2}(\bar{n} + 1)(2\sigma_- \tilde{\rho} \sigma_+ - \sigma_+ \sigma_- \tilde{\rho} - \tilde{\rho} \sigma_+ \sigma_-) \\ & + \frac{\gamma}{2}\bar{n}(2\sigma_+ \tilde{\rho} \sigma_- - \sigma_- \sigma_+ \tilde{\rho} - \tilde{\rho} \sigma_- \sigma_+). \end{aligned} \quad (4.60)$$

Equation (4.60) is the master equation in thermal equilibrium. In the Schrödinger picture, Eq.(4.60) will becomes

$$\begin{aligned} \dot{\rho} = & -i\frac{1}{2}(w_A + 2\Delta' + \Delta)[\sigma_z, \rho] + \frac{\gamma}{2}(\bar{n} + 1)(2\sigma_- \rho \sigma_+ - \sigma_+ \sigma_- \rho - \rho \sigma_+ \sigma_-) \\ & + \frac{\gamma}{2}\bar{n}(2\sigma_+ \rho \sigma_- - \sigma_- \sigma_+ \rho - \rho \sigma_- \sigma_+). \end{aligned} \quad (4.61)$$

Compared with Liouville-Von Neumann in the close system the equation of motion for density matrix, Eq(4.61) has two extra dissipative parts coming from interacting with the environment. In addition, the frequency w_A in Eq.(4.61) becomes to $w_A + 2\Delta' + \Delta$.

4.2.2 Dephasing

In above section, we use the interaction, Eq.(4.38), to obtain the master equation in thermal equilibrium. However, the thermal and vacuum fluctuations in the environment may also cause the off-diagonal component of the density matrix to decay in time without changing the population in each state. This is called a dephasing process. To account for this addition dephasing process, interaction.

We add phenomenologically a reservoir interaction

$$H_{dephasing} = H_{R_1} + H_{SR_1}, \quad (4.62)$$

$$H_{R_1} = \sum_k \hbar w_k \gamma_k^\dagger \gamma_k, \quad (4.63)$$

$$H_{SR_1} = \sum_{j,k} \hbar (\kappa_{jk}^* \gamma_k^\dagger \sigma_z + \kappa_{jk} \gamma_j \sigma_z) \quad (4.64)$$

$$(4.65)$$

Using the similar method in the previous section, we can get

$$\tilde{s}_3(t) = \sigma_- \sigma_+, \quad (4.66)$$

$$\tilde{s}_4(t) = \sigma_+ \sigma_-, \quad (4.67)$$

$$\tilde{\Gamma}_3(t) = \sum_{j,k} \kappa_{jk}^* \gamma_j^\dagger e^{i w_k t}, \quad (4.68)$$

$$\tilde{\Gamma}_4(t) = \sum_{j,k} \kappa_{jk} \gamma_j e^{i w_k t}, \quad (4.69)$$

Thus we just need to add the extra terms form interaction $\tilde{\Gamma}_3$ and $\tilde{\Gamma}_4$. We can obtain the dephasing part of the master equation using a method similar to that of obtaing

Eq.(4.61),

$$\begin{aligned}
\dot{\rho}_{dephase} = & - \int_0^\infty [\sigma_z \sigma_z \tilde{\rho}(t') - \sigma_z \tilde{\rho}(t') \sigma_z] \langle \tilde{\Gamma}_3(t) \tilde{\Gamma}_3(t') \rangle_{R_1} \\
& + [\tilde{\rho}(t') \sigma_z \sigma_z - \sigma_z \tilde{\rho}(t') \sigma_z] \langle \tilde{\Gamma}_3(t') \tilde{\Gamma}_3(t) \rangle_{R_1} \\
& + [\sigma_z \sigma_z \tilde{\rho}(t') - \sigma_z \tilde{\rho}(t') \sigma_z] \langle \tilde{\Gamma}_4(t) \tilde{\Gamma}_4(t') \rangle_{R_2} \\
& + [\tilde{\rho}(t') \sigma_z \sigma_z - \sigma_z \tilde{\rho}(t') \sigma_z] \langle \tilde{\Gamma}_4(t') \tilde{\Gamma}_4(t) \rangle_{R_2}.
\end{aligned} \tag{4.70}$$

Similarly, we assume that the reservoir correlation time are much shorter than the system dynamics, so Eq.(4.70) becomes to

$$\dot{\rho}_{dephase} = -\frac{i}{2} \Delta_p [\sigma_z, \tilde{\rho}] + \frac{\gamma_p}{2} (\sigma_z \tilde{\rho} \sigma_z - \tilde{\rho}), \tag{4.71}$$

where both coefficients, γ_p and Δ_p , depend on the thermal reservoir. Equation (4.71) thus the total equation of motion in the Schrödinger picture can be written as

$$\begin{aligned}
\dot{\rho} = & - \frac{i}{2} w'_A [\sigma_z, \rho] + \frac{\gamma}{2} (\bar{n} + 1) (2\sigma_- \rho \sigma_+ - \sigma_+ \sigma_- \rho - \rho \sigma_+ \sigma_-) \\
& + \frac{\gamma}{2} \bar{n} (2\sigma_+ \rho \sigma_- - \sigma_- \sigma_+ \rho - \rho \sigma_- \sigma_+) + \frac{\gamma_p}{2} (\sigma_z \rho \sigma_z - \rho),
\end{aligned} \tag{4.72}$$

where

$$w'_A = w_a + 2\Delta' + \Delta + \Delta_p, \tag{4.73}$$

with Δ' and Δ given in the previous section. In the next chapter we will use the dephasing model to describe the motion of the system in the silicon-base donor spin quantum computer as the dephasing process may be the dominant source of decoherence in that system.

Chapter 5

Optimal Control in Open Quantum Systems

5.1 Introduction

The criteria necessary for any quantum computer including:

- (1) Well defined quantum bits (Qubits) in the system.
- (2) The initial states can be prepared such as: $|00\dots\rangle$.
- (3) The gate operation time is shorter than decoherence time.
- (4) The universal set of quantum gates can be constructed.
- (5) Measurement of qubits can be performed.

Hence, one of the important criteria for a practical quantum computer is the construction of quantum gates with operation times much shorter than relevant decoherence time. In addition, high-fidelity quantum gates are also desired for fault-tolerant quantum computation. The fidelity is defined as $Tr(G^\dagger U)$, where the G is the desired quantum gate U is the quantum gate in practice, and the error is defined as $1 - Tr(G^\dagger U)$. The error threshold required for fault-tolerant quantum computation is about $10^{-3} \sim 10^{-4}$ [13]. Therefore, fast and high-fidelity quantum gates are desired. We can use the optimal control theory, the Krotov method, to find out the near time optimal. We may choose a time interval and use Krotov method to see whether we can find the control sequence of the quantum gate which satisfies the required fidelity

in this time interval. If yes, we can choose a shorter time interval to repeat the calculation. If not, we can choose a longer time interval to repeat the calculation. Then, we can find a control sequence and using it to find out a quantum gate which satisfies the required fidelity with the shortest time interval. In the following sections, we will detail how to use the Krotov method to find out the near time-optimal control sequence for a Hadmard gate.

5.2 Krotov Method in Density Matrix

5.2.1 Equation of Motion

We consider an open quantum system and the density matrix, ρ of the subsystem of interest, has $N \times N$ dimensions. The equation of motion for density matrix can be written as

$$\begin{aligned}\dot{\rho}(t) &= -\frac{i}{\hbar}[H_S, \rho] + \Gamma\rho, \\ &= \mathcal{M}\rho,\end{aligned}\tag{5.1}$$

$$\Rightarrow \dot{\rho}^c(t) = \mathcal{L}\rho^c\tag{5.2}$$

where H_S is the full Hamiltonian of the subsystem, the superoperator Γ denotes the decoherence effect and \mathcal{M} the Liouville superoperator. Also in Eq.(5.2), we change the density matrix to a column vector and \mathcal{L} is the corresponding matrix.

Equation(5.1) is the equation of motion for the density matrix or Eq.(5.2) is the equation of motion for density column. We, however, want to get the equation of motion for an operator evolution, so we use Eq.(5.2) and the relation $\rho^c(t) = U\rho^c(0)$ to

$$\begin{aligned}\frac{d}{dt}(U(t)\rho^c(0)) &= \mathcal{L}U(t)\rho^c(0), \\ \dot{U}(t)\rho^c(0) &= \mathcal{L}U(t)\rho^c(0), \\ \Rightarrow \dot{U}(t) &= \mathcal{L}U(t).\end{aligned}\tag{5.3}$$

Although, the Eq.(5.3) is the equation of motion for the operator revolution, its variables have real and imaginary parts. The Krotov method is developed in the real

space. Therefore, we separate the equation of motion into two real functional. First, we transform Eq.(5.3) into a different form with a matrix \mathcal{L}^m and a column U^c such that the expression $\dot{U}^c = \mathcal{L}^m U^c$ describes the same equation of motion as Eq.(5.3), i.e.,

$$\begin{aligned} \dot{U}(t) &= \mathcal{L}U(t), \\ \Rightarrow \dot{U}^c(t) &= \mathcal{L}^m U^c(t), \end{aligned} \quad (5.4)$$

where U^c is a column vector and \mathcal{L}^m is a matrix. Then, we can define that

$$U^c = U_R^c + iU_I^c, \quad (5.5)$$

where U_R^c and U_I^c are real and imaginary part of the column vector, U^c . In addition, we define

$$\mathcal{L}^m = \Omega_R + i\Omega_I, \quad (5.6)$$

where Ω_R and Ω_I are real matrices corresponding to the real and imaginary parts of the matrix \mathcal{L}^m . Inserting Eq.(5.5) and (5.6) back into the Eq.(5.4), we obtain

$$\begin{aligned} \dot{U}_R^c + i\dot{U}_I^c &= (\Omega_R + i\Omega_I)(U_R^c + iU_I^c), \\ \Rightarrow \dot{U}_R^c &= f_R = \Omega_R U_R^c - \Omega_I U_I^c, \end{aligned} \quad (5.7)$$

$$\Rightarrow \dot{U}_I^c = f_I = \Omega_I U_R^c + \Omega_R U_I^c. \quad (5.8)$$

It should be mentioned that because the dimension of the density matrix is $N \times N$, when we use transformed Eq.(5.4), the dimension of the corresponding superoperator, \mathcal{L} will become $N^2 \times N^2$, thus the operator U also is $N^2 \times N^2$. In addition, we use transformed Eq.(5.4), the dimension of the operator will become $N^4 \times N^4$. Also, if the equation of motion for operator evolution has $N^2 \times N^2$ dimension, we will have $2N^2 \times N^2$ real functionals to describe the equation of motion. Another point is that the control parameter is in the superoperator \mathcal{L} (\mathcal{L}^m , or in both real matrices Ω_R and Ω_I). It means that both real matrices Ω_R and Ω_I are functional of time and the control.

5.2.2 Goal Functional

Following the descriptions in the previous section and in chapter 2, we use the Krotov method to find the minimum value of the goal functional

$$I[U_R^c(t), U_I^c(t), \epsilon, t] = F[U_R^c(T), U_I^c(T)] + \int_0^T f^0[U_R^c(t), U_I^c(t), t] dt, \quad (5.9)$$

where the U_R^c and U_I^c are a $2 \times N^2$ -dimensional column vector, and ϵ is the control parameter. In the Krotov method, both functionals $F[U_R^c(T), U_I^c(T)]$ and $f^0[U_R^c(t), U_I^c(t), t]$ in the goal functional are real functionals. However, the quantum system is in a complex Hilber space, so in general, the goal functional is complex. In our case we want to find the minimum value of the error defined as

$$\begin{aligned} E &= 1 - \text{Tr}[G^\dagger U(T, 0, \epsilon)], \\ &= 1 - \tau(G; T; \epsilon), \end{aligned} \quad (5.10)$$

where G is the desired quantum gate, $U(T)$ is the final time quantum gate operation which is obtained from the optimal control sequence and the equation of motion for the operator evolution. So the error functional is complex. Also, the functional $\tau(G; T; \epsilon)$ defined as fidelity is a complex number restricted to the interior of a circle with a radius N centered at the origin in the complex plane. The modulus of τ is equal to N only for an optimal control operation satisfying

$$U(T, 0; \epsilon) = e^{-i\varphi(T)} G, \quad (5.11)$$

where $\varphi(T)$ is a global phase. When τ approaches N , the transformation imposed by the field converges to the goal quantum gate. Although the functional τ is complex, we can separate several different real functionals can be associated whit it. In [8], the optimization of the real part of τ , or the imaginary part, or a linear combination of both was suggested to find the optimal control. In this thesis, the real part

$$F_R = -\text{Re}[\tau(G; T; \epsilon)] = -\text{Re}[\text{Tr}(G^\dagger U(T, 0, \epsilon))], \quad (5.12)$$

was chosen. The functional reaches its minimum value, $F_R = -N$, when the control induces the goal quantum gate but with the additional condition that the phase term

$e^{-i\phi(T)}$ is equal to one. Another functional based on τ but without any condition on the phase can be defined. In this work the squared modulus of τ with a negative sign is studied:

$$\begin{aligned} F_{sm} &= -|\tau(G; T; \epsilon)|^2, \\ &= -Tr[G^\dagger U(T, 0, \epsilon)]Tr[G^\dagger U(T, 0, \epsilon)]^*, \end{aligned} \quad (5.13)$$

with minimum value $F_{sm} = -N^2$ when the control induces the goal quantum gate. In our case, we can define the functional f^0 to be 0. Therefore, the goal functional $I[U_R^c(t), U_I^c(t), \epsilon, t]$, Eq.(5.9), can be defined as

$$I[U_R^c(t), U_I^c(t), \epsilon, t] = 1 - \tau(G; T; \epsilon). \quad (5.14)$$

5.2.3 Decompose the goal functional in Quantum System

In the Krotov method, we will decompose the goal functional into two parts by the functional ϕ , where the two parts include the functionals R and G. In this section, we will introduce ϕ , R and G functionals in the quantum system. The functional ϕ depends on time and the evolution of the system. According to Eq.(3.23), Eq.(3.25) and the condition Eq.(3.28), we can write

$$\left\{ \begin{aligned} \dot{\Phi}_R[t, U_R^{ci}, U_I^{ci}(t)] &= -J_R^T(t)\Phi_R(t) - J_I^T\Phi_I(t) + \frac{\partial}{\partial U_R^c} f^0(t, U_R^{c0}, U_I^{c0}, \epsilon^0), \\ \dot{\Phi}_I[t, U_R^{ci}, U_I^{ci}(t)] &= J_I^T(t)\Phi_R(t) - J_R^T(t)\Phi_I(t) + \frac{\partial}{\partial U_I^c} f^0(t, U_R^{c0}, U_I^{c0}, \epsilon^0), \\ \phi[t, U_R^{ci}, U_I^{ci}(t)] &= \Phi_{iR}(t)U_R^{ci} + \Phi_{iI}(t)U_I^{ci} \\ &\quad + 0.5\sigma_{iR}(t)(\Delta U_R^{ci})^2 + 0.5\sigma_{iI}(t)(\Delta U_I^{ci})^2, \quad (i = 1, 2, \dots, n) \end{aligned} \right.$$

Using the definition of J , Eq.(3.24), the fact that the equations of motion, Eq.(5.7) and Eq.(5.8) just depend on only the first power of U_R^{ci} or U_I^{ci} , we obtain

$$J_R = \Omega_R, \quad (5.15)$$

$$J_I = \Omega_I. \quad (5.16)$$

Also, in our case, the functional f^0 is 0, and we can get

$$\dot{\Phi}_R(t) = -\Omega_R^T \Phi_R - \Omega_I^T \Phi_I, \quad (5.17)$$

$$\dot{\Phi}_I(t) = \Omega_I^T \Phi_R - \Omega_R^T \Phi_I, \quad (5.18)$$

$$\Phi_R(T) = \frac{\partial}{\partial U_R^{ci}}(\tau(G; T; \epsilon)), \quad (5.19)$$

$$\Phi_I(T) = 0. \quad (5.20)$$

Then we can use Eq.(3.3) and Eq.(3.4) to obtain

$$R[t, U_R^{ci}, U_I^{ci}, \epsilon] = \frac{\partial \phi}{\partial U_R^{ci}} f_R + \frac{\partial \phi}{\partial U_I^{ci}} f_I - \frac{\partial \phi}{\partial t}, \quad (5.21)$$

$$G[T, U_R^{ci}(T), U_I^{ci}(T)] = F_R + \phi[T, U_R^{ci}(T), U_I^{ci}(T)], \quad (5.22)$$

$$= -Re[Tr(G^\dagger U(T, 0, \epsilon))] + \phi[T, U_R^{ci}(T), U_I^{ci}(T)]. \quad (5.23)$$

We have constructed real and imaginary parts of the functional Φ , functional R , and functional G for the quantum system. By following the algorithm of the Krotov method, we can then find out the optimal control sequence for quantum gate $U(T)$.

5.3 In Silicon-base Donor Spin Quantum Computer

5.3.1 System

We use the silicon-based electron spin quantum computing architecture discussed in Chapter 2 to be our system. Because the rotation magnetic field is always on in this scheme, electron will undergo a rotating around the x-axis when there are no voltages applied on A gates, i.e. $\Delta w = 0$ with an angular frequency of $\omega_0 = g_e \mu_B B_{ac} / \hbar$. While target electrons will perform a particular operation with time t , every spectator qubit will rotate with an angle of $\theta_x = -\omega_0 t$. If the angle θ_x equal to $2n\pi$, where n is integral, then we don't need any correction step for spectator qubits. Different gate operation time t will require different B_{ac} . We choose $n = 1$ to minimize the time, and obtain

$$B_{ac} = \frac{2\pi\hbar}{g_e \mu_B t}, \quad (5.24)$$

where t is the gate operation time. In general, decoherence may cause by two different processes: includes two part: dephasing and relaxation. According to experiment, however, dephasing is the dominant source of decoherence for silicon-base donor spin quantum computer. For example, Feher and Gere [9] measured the energy relaxation time, T_1 , $T_{1n} > 10$ hours for nuclear spin and $T_{1e} \approx 30$ hours for electron spin at a temperature of $T = 1.25K$, $B = 3.2T$. In contrast, experimentally measured dephasing time, T_2 , is much shorter. Gordon and Bowers [10] measured $T_{2e} = 520\mu s$ for P:Si at $T = 1.4K$. Chiba and Harai [11] also measured the electronic dephasing times of P:Si, finding a time of $T_{2e} = 100\mu s$. Recently, Tyryshkin et al. [12] experimentally measured the decoherence time T_{2e} of electron spins for a donor concentration of isotopically purified ^{28}Si , and obtain a value $T_{2e} \approx 62\text{ms}$ at $T = 6.9K$. Therefore, we assume that the only decoherence present in the system is dephasing. Using the master equation

$$\dot{\rho} = -\frac{i}{\hbar}[H_s, \rho] - \Gamma\rho, \quad (5.25)$$

where H_s is full Hamiltonian,

$$H_S = \sum_{i=1}^2 H_{B_i} + H_{A_i} + H_J + H_{AC_i}, \quad (5.26)$$

$$H_{B_i} = \frac{1}{2}g_e\mu_B B_0\sigma_z^{ie} - \frac{1}{2}g_n\mu_n B_0\sigma_z^{in}, \quad (5.27)$$

$$H_{A_i} = A_1\sigma^{ie} \cdot \sigma^{in}, \quad (5.28)$$

$$H_J = J\sigma^{1e} \cdot \sigma^{2e}, \quad (5.29)$$

$$H_{AC_i} = \frac{1}{2}g_e\mu_B B_{ac}(\cos(w_{act})(\sigma_x^{ie}) + \sin(w_{act})(\sigma_y^{ie})) \\ - \frac{1}{2}g_n\mu_n B_{ac}(\cos(w_{act})(\sigma_x^{in}) + \sin(w_{act})(\sigma_y^{in})) \quad (5.30)$$

and the $\Gamma\rho$ is dephasing term.

$$\Gamma\rho = \sum_{i=1}^2 \Gamma_e[Z_{e_i}, [Z_{e_i}, \rho]] + \Gamma_n[Z_{n_i}, [Z_{n_i}, \rho]], \quad (5.31)$$

Where Γ_n is the nuclear dephasing rate and Γ_e the electronic dephasing rate. The dephasing rate, Γ_n and Γ_e are related to the dephasing times by

$$\Gamma_e = \frac{1}{4T_{2e}}, \quad (5.32)$$

$$\Gamma_n = \frac{1}{4T_{2n}}. \quad (5.33)$$

Here, we use the value of 60ms [12] as a conservative estimate for electronic dephasing times. Additionally, we expect the nuclear spin dephasing times is much longer than electronic dephasing times. Hence, the value of dephasing rate of the nuclear spin can be approximated to 0 where compared with electron spin T_{2e}^{-1} and the inverse of gate the operation time. Thus, in the condition $\Gamma_n \approx 0$, Eq.(5.25) becomes to

$$\dot{\rho} = -\frac{i}{\hbar}[H_s, \rho] - \sum_{j=1}^2 \Gamma_e[Z_{e_j}, [Z_{e_j}, \rho]]. \quad (5.34)$$

We can go to the rotating frame which rotates with the frequency of the rotating magnetic field, and use the relation

$$\tilde{\rho} = U_{rot}\rho U_{rot}^\dagger, \quad (5.35)$$

$$U_{rot} = e^{\frac{i}{2}w_{ac}\sigma_z t}, \quad (5.36)$$

where w_{ac} is the frequency of the rotating magnetic field. Substituting Eq.(5.35) into the Eq.(5.1), we can get the equation of motion of density matrix in the rotation frame

$$\dot{\tilde{\rho}}(t) = -\frac{i}{\hbar}[\tilde{H}_S, \tilde{\rho}] - \sum_{j=1}^2 \Gamma_e[Z_{e_j}, [Z_{e_j}, \tilde{\rho}]], \quad (5.37)$$

where the \tilde{H}_S is the reduced Hamiltonian,

$$\tilde{H}_S = \sum_{i=1}^2 \frac{\hbar}{2} \Delta w_i \sigma_z^i + \frac{1}{2} g_e \mu_B B_{ac} \sigma_x^i + J \sigma^{1e} \cdot \sigma^{2e}, \quad (5.38)$$

$$\Delta w = \frac{1}{\hbar} \left(2A - 2A_0 + \frac{2A^2 - 2A_0^2}{\frac{1}{2}g_e\mu_B B_0 + \frac{1}{2}g_n\mu_n B_0} \right). \quad (5.39)$$

Equation (5.37) is the equation of motion for the density matrix. However, we want to get the equation of motion for quantum gate the operator. Hence, first

we change the arrangement of the density matrix into a column vector. A useful transformation relation is

$$A \begin{pmatrix} \rho_{11} & \rho_{12} & \cdots & \rho_{1n} \\ \rho_{21} & \rho_{22} & \cdots & \rho_{2n} \\ \vdots & \vdots & \ddots & \vdots \\ \rho_{n1} & \rho_{n2} & \cdots & \rho_{nn} \end{pmatrix} B \implies A \otimes B^T \begin{pmatrix} \rho_{11} \\ \rho_{12} \\ \vdots \\ \rho_{1n} \\ \rho_{21} \\ \vdots \\ \rho_{nn} \end{pmatrix}, \quad (5.40)$$

where A and B are arbitrary matrices and B^T is the transpose of the matrix B . Using above relation, we can define the superoperator \mathcal{L}

$$\begin{aligned} \dot{\tilde{\rho}}(t) &= -\frac{i}{\hbar}[\tilde{H}_S, \tilde{\rho}] - \sum_{j=1}^2 \Gamma_e[Z_{e_j}, [Z_{e_j}, \tilde{\rho}]], \\ \implies \dot{\tilde{\rho}}^c(t) &= \mathcal{L}\rho^c, \end{aligned} \quad (5.41)$$

where ρ^c is the density column vector arranged as Eq.(5.40). Also, we can use Eq.(5.3) to obtain the equation of motion for the quantum gate operator and the analytical solution of Eq.(5.7) and Eq.(5.8).

5.3.2 Hadamard Gate

In this section, we will apply the Krotov optimization method. To find a high-fidelity Hadamard gate. The Hadamard gate is a single-qubit gate and is defined as:

$$H = \frac{1}{\sqrt{2}} \begin{pmatrix} 1 & 1 \\ 1 & -1 \end{pmatrix}. \quad (5.42)$$

The gate turns a $|0\rangle$ into a $(|0\rangle + |1\rangle)/\sqrt{2}$ state and turns a $|1\rangle$ state into a $(|0\rangle - |1\rangle)/\sqrt{2}$ state. Figure 5.1 is a schematic illustration of a Hadamard gate quantum circuit.

We consider a single-qubit case, so the index j just needs to be 1 in Eq.(5.41) and

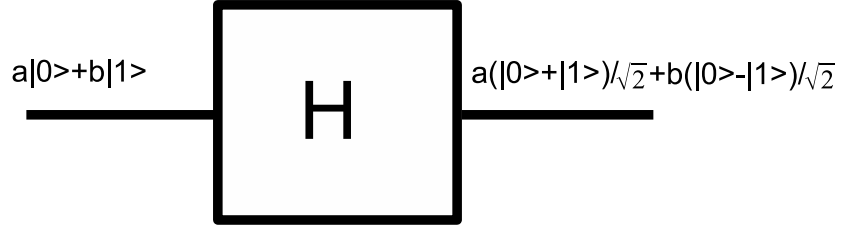


Figure 5.1: The symbol of the quantum circuit for Hadamard

Eq.(5.38)

$$\begin{aligned}
 \dot{\tilde{\rho}}(t) &= -\frac{i}{\hbar}[\tilde{H}_S, \tilde{\rho}] - \Gamma_e[Z_{e_1}, [Z_{e_1}, \tilde{\rho}]], \\
 &= -\frac{i}{\hbar}(\tilde{H}_S \tilde{\rho} - \tilde{\rho} \tilde{H}_S) - 2\Gamma_e \tilde{\rho} + 2\Gamma_e Z_{e_1} \tilde{\rho} Z_{e_1},
 \end{aligned} \tag{5.43}$$

where

$$\tilde{H}_S = \frac{\hbar}{2} \Delta w_1 \sigma_z^1 + \frac{1}{2} g_e \mu_B B_{ac} \sigma_x^1, \tag{5.44}$$

and Δw has the same expression as Eq.(5.39). Using the relation of Eq.(5.40), we may obtain

$$\mathcal{L} = -\frac{i}{\hbar}(\tilde{H}_S \otimes I^T - I \otimes \tilde{H}_S^T) - 2\Gamma_e I \otimes I^T + 2\Gamma_e Z_{e_1} \otimes Z_{e_1}^T, \tag{5.45}$$

where I is the identity matrix. Therefore, we find the superoperator, \mathcal{L} , in Eq.(5.3). Using the relation(5.40) again to obtain the superoperator, \mathcal{L}^m , in the Eq.(5.4). Also, we can use Eq.(5.5) and Eq.(5.6) to obtain the equaiton of motion for quantum gate operator in the real functional form. The flow chart for getting the equaiton of motion for quantum gate operator in the real function form is shown in Fig.5.2

Because when we find out the equation of motion we have changed the arrangement of the density matrix, we need to change the form of the Hardmard gate in

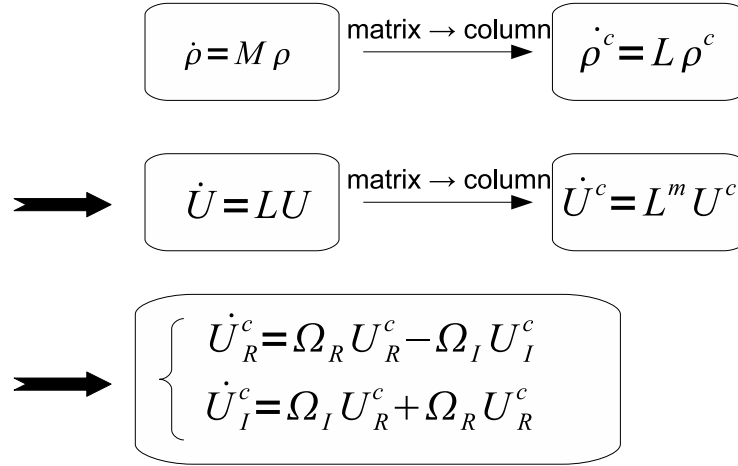


Figure 5.2: The step for finding out the equation of motion for operator in real functional.

the goal functional using Eq.(5.40). First, we need to understand the function of the Hadmard gate acting on the density matrix

$$\begin{aligned}
 |\phi\rangle &\Rightarrow H|\phi\rangle, \\
 \rho = |\phi\rangle\langle\phi| &\Rightarrow H|\phi\rangle\langle\phi|H^\dagger = H\rho H^\dagger,
 \end{aligned}
 \tag{5.46}$$

According to the flow chart, we have chaged the density matrix to the column vector form with the relation, Eq.(5.40), so we should with the same relation to find the Hadmard matrix for the density column vector. Using Eq.(5.40), we obtain

$$\begin{aligned}
 &H\rho H^\dagger \\
 \Rightarrow &\left[\frac{1}{\sqrt{2}} \begin{pmatrix} 1 & 1 \\ 1 & -1 \end{pmatrix} \right] \begin{pmatrix} \rho_{11} & \rho_{12} \\ \rho_{21} & \rho_{22} \end{pmatrix} \left[\frac{1}{\sqrt{2}} \begin{pmatrix} 1 & 1 \\ 1 & -1 \end{pmatrix} \right] \\
 \Rightarrow &\frac{1}{2} \begin{pmatrix} 1 & 1 & 1 & 1 \\ 1 & -1 & 1 & -1 \\ 1 & 1 & -1 & -1 \\ 1 & -1 & -1 & 1 \end{pmatrix} \begin{pmatrix} \rho_{11} \\ \rho_{12} \\ \rho_{21} \\ \rho_{22} \end{pmatrix},
 \end{aligned}
 \tag{5.47}$$

and the Hadamard matrix in the density column vector representation is

$$\frac{1}{2} \begin{pmatrix} 1 & 1 & 1 & 1 \\ 1 & -1 & 1 & -1 \\ 1 & 1 & -1 & -1 \\ 1 & -1 & -1 & 1 \end{pmatrix}. \quad (5.48)$$

We can use the definition of the fidelity or error, Eq.(5.10) and Eq.(5.12) to obtain the goal functional

$$\begin{aligned} I[U, \epsilon, t] &= -Re[Tr(G^\dagger U(T, 0, \epsilon))] \\ \Rightarrow I[U_R^c, \epsilon, t] &= -\frac{1}{8}(U_{R1}^c + U_{R2}^c + U_{R3}^c + U_{R4}^c + U_{R5}^c - U_{R6}^c + U_{R7}^c \\ &\quad - U_{R8}^c + U_{R9}^c + U_{R10}^c - U_{R11}^c - U_{R12}^c + U_{R13}^c - U_{R14}^c \\ &\quad - U_{R15}^c + U_{R16}^c), \end{aligned} \quad (5.49)$$

where U_{Ri}^c means the i-th component in the real part column, U_R^c . Now, we have equation of motion and goal functional then we can implement the Krotov optimization method.

5.4 Result

We use silicon-base donor spin quantum computer architecture discussed in chapter 2 to be our system, and we follow the previous section to obtain following result.

Figure 5.3 shows the optimal fidelity versus the gate operation time resulting from the Krotov method. The best fidelity is about 0.9993 or error 7×10^{-4} for the operation time of 12.35 ns. The error is below the error threshold of 10^{-3} [12].

We consider the rate of convergence for the Krotov method in open quantum system. According to Fig. 5.4, we can obtain the optimal solution (the best fidelity) when we repeat the algorithm three times.

The parameter A in Eq.(2.17) is our control parameter to implement a Hadamard gate and the range of the parameter A is between 1.211×10^{-7} eV and 0.606×10^{-7} eV. Using the Krotov method, we obtain the control sequence shows in Fig. 5.5, for the near time-optimal, high-fidelity Hadamard gate.

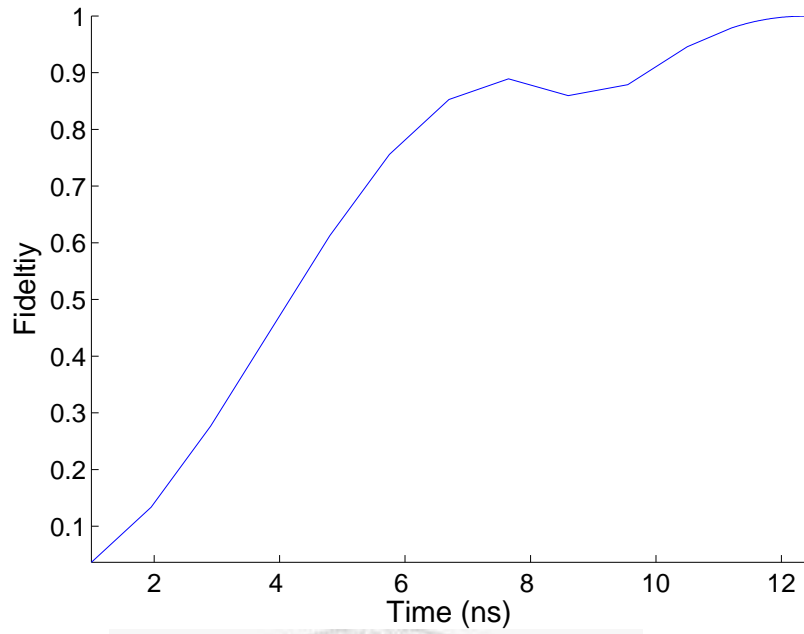


Figure 5.3: Relation of the optimal fidelity versus the gate operation time. The highest fidelity occur at the gate operation time of 12.35ns

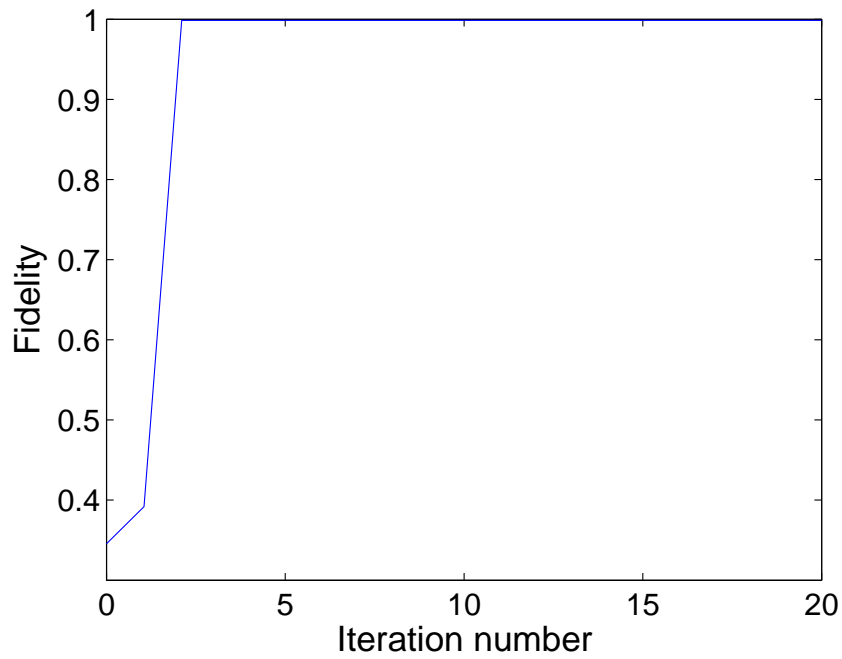


Figure 5.4: Relation of iteration number and the fidelity. We pick the gate operation time of 12.16ns

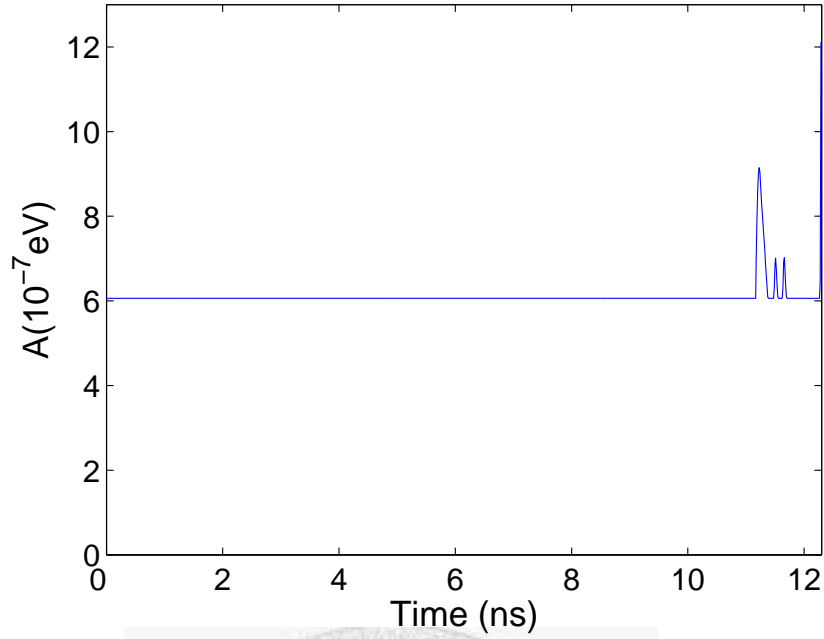


Figure 5.5: The control sequence and the result from Krotov method

We use the control sequence in Fig. 5.5 to check the state evolution, and we define the state $|1\rangle$ as the spin-up state and $|0\rangle$ as the spin-down. Figure 5.6, shows the result of the time evolution of the probability of finding the electron spin (a) in state $|1\rangle$ (b) in state $|0\rangle$ for an initial state $|1\rangle$ using the Hadamard gate sequence of Fig. 5.5. From Fig. 5.6, we see that if the initial state is $|1\rangle$, after the application of the control sequence of Fig. 5.5, the donor electron spin has a probability $1/2$ to be in state $|1\rangle$ and probability $1/2$ in state $|0\rangle$. Similar, we check the other cases, including the initial states $|0\rangle$, $1/\sqrt{2}(|1\rangle + |0\rangle)$ and $1/\sqrt{2}(|1\rangle - |0\rangle)$. These result are shown in Fig. 5.7, Fig. 5.8 and Fig.5.9, respectively. For an initial state $|0\rangle$ the donor electron spin has $1/2$ probability to evolve to $|0\rangle$ and $|1\rangle$, as shown in Fig. 5.7. If the initial state is $1/\sqrt{2}(|1\rangle + |0\rangle)$ it will evolve to $|1\rangle$, shown in Fig. 5.8. On the other hand, if the initial state is $1/\sqrt{2}(|1\rangle - |0\rangle)$, it, will evolve to $|0\rangle$, shown in Fig. 5.9.

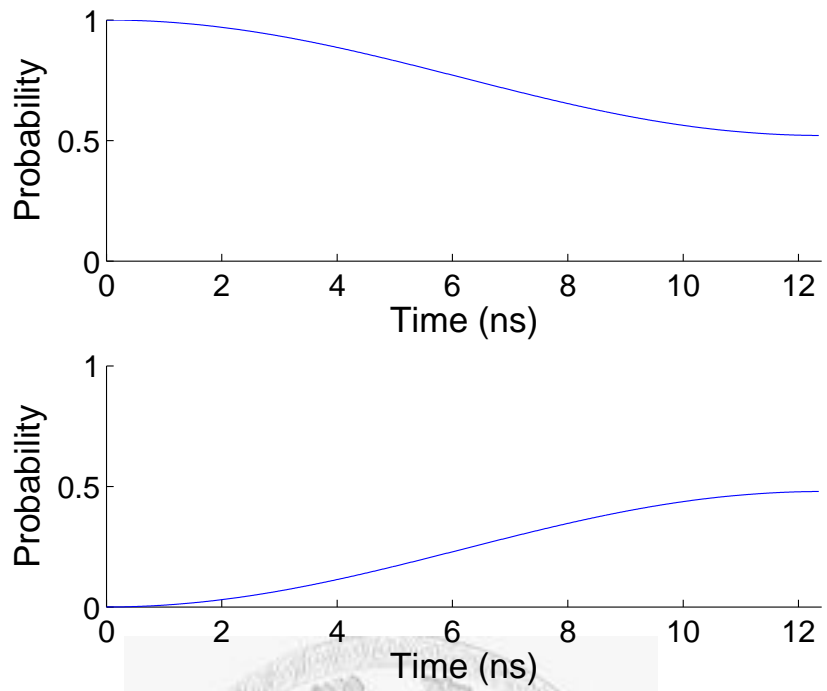


Figure 5.6: State probability evolution of the Hadamard gate for an initial state $|1\rangle$

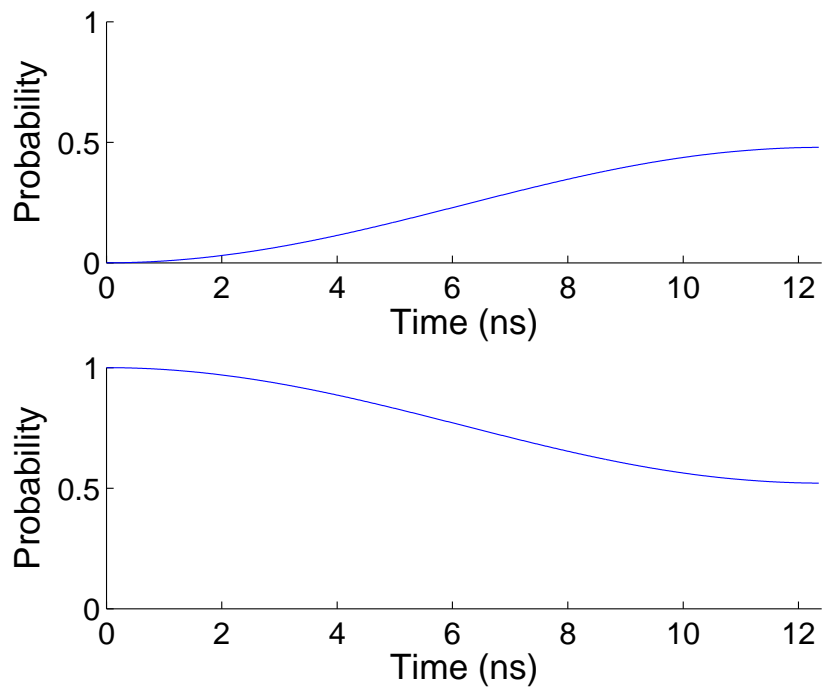


Figure 5.7: State probability evolution of the Hadamard gate for an initial state $|0\rangle$

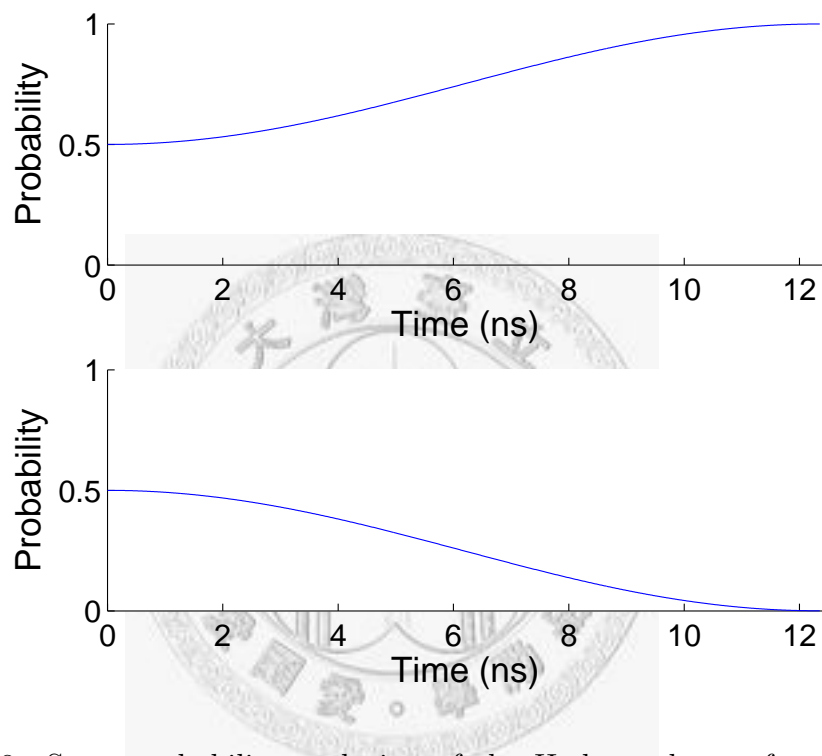


Figure 5.8: State probability evolution of the Hadamard gate for an initial state $\frac{1}{\sqrt{2}}(|1\rangle + |0\rangle)$

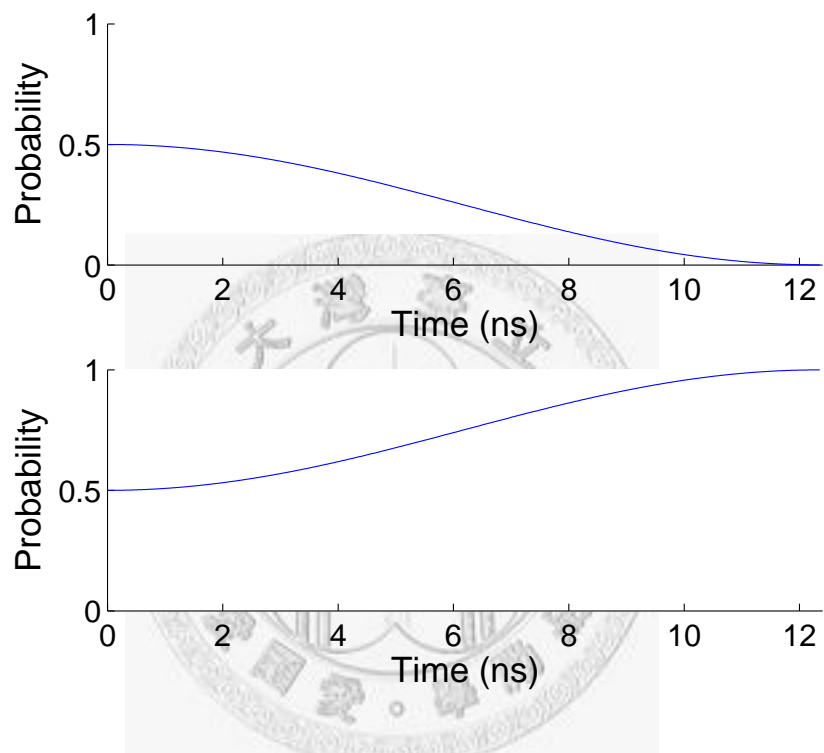


Figure 5.9: State probability evolution of the Hadamard gate for an initial state $\frac{1}{\sqrt{2}}(|1\rangle - |0\rangle)$

Chapter 6

Conclusion

This thesis was primarily concerned with the Krotov method for obtaining near time-optimal and high-fidelity control sequence for quantum gate operations in open quantum system. We explicitly find the optimal control sequence for Hadamard gate for the Kane silicon-based donor spin quantum computing.

We have given our motivation to study this problem and have described the Hamiltonian for the silicon-base donor spin quantum computing. We have also analyzed the control processes and given the equation of motion for an ideal unitary case. We have described the basic idea of the Krotov method, a general method for optimal control problem. The advantage of the Krotov method is that for implementing the Krotov method, we just need to know the equation of motion of the system, and the Krotov method can deal with a large dimension vector space. We have given simple two examples to illustrate the use of the Krotov optimization method. One is a discrete problem with a goal functional depending on just the final time and the other is a continuous in time problem. We have also introduced the master equation approach to describe open quantum systems under the Born-Markoff approximation. We have derived the master equation for a two-state system in a thermal equilibrium environment. To study the optimal control for the silicon-base donor spin quantum computing we have detailed the Krotov method for obtaining optimal quantum gate operations in an open quantum system. Using a dephasing model to obtain the equation of motion for our system, we have applied the Krotov method to obtain the near

time-optimal and high-fidelity control sequence for a Hadamard gate. The operation time of 12.35 ns with 7×10^{-4} error which is below the error threshold of 10^{-3} [13] required for the fault-tolerant quantum computation. The Krotov method may prove useful in implementing quantum gate operations in real quantum computing experiments in the future.



Bibliography

- [1] D.Deutsch. Quantum Theory, the Church-Turing thesis and the Universal Quantum Computer. Proc. Royal Soc. of London A400, 97(1985).
- [2] B.E. Kane. A Silicon-Based Nuclear Spin Quantum Computer. Nature 393, 133(1998).
- [3] C. D. Hill, Ph.D thesis (University of Queensland, Brisbane, Australia, 2006).
- [4] C. Herring and Flicker, "Asymptotic Exchange Coupling of two Hydrogen Atom", Phys. Rev. 134, A362-A366(1964).
- [5] V.F. Krotov, Global Methods in Optimal Control Theory(Dekker,New York,1996)
- [6] A.I. Konnov and V.F. Krotov, Automation and Remote Control Vol. 60, No. 10, 1999
- [7] A.I. Propoi, Elements of the Theory of Optimal Discrete Systems, Nauka, Moscow (1981) (in Russian)
- [8] J.P. Palao and R. Kosloff, Phys. Rev. Lett. 89, 188301(2002)
- [9] G. Feher and E.A. Gere. Electron Spin Resonance Experiments on Donor in Silicon. II. Electron Spin Relaxtion Effect. Phys. Rev. 114(4),1245(1959)
- [10] J.P. Gordon an K.D. Bowers. Microwave Spin Echoes From Donor Electrons in Silicon. Phys Rev. Lett 1(10)(1958)

- [11] M.Chiba and A. Hirai. Electron Spin Echo Decay Behaviours of Phosphorus Doped Silicon. J. Phys. Soc. Japan 33(3),730 (1972)
- [12] A.M. Tyryshkin, S.A. Lyon, A.V. Astashkin, and A.M. Raitsimring. Electron Spin-Relaxation Times of Phosphorus donors in Silicon. Phys. Rev B 68, 193207(2003)
- [13] P. Aliferis and J. Preskill, Phys. Rev. A 79,012332(2009)



Appendix A

Changing a Matrix to a Column

We first consider a simple matrix multiplication of three 2×2 square matrices. Our goal is to change the middle matrix from a matrix to a column vector, in a form shown below.

$$ABC = \begin{pmatrix} a_{11} & a_{12} \\ a_{21} & a_{22} \end{pmatrix} \begin{pmatrix} b_{11} & b_{12} \\ b_{21} & b_{22} \end{pmatrix} \begin{pmatrix} c_{11} & c_{12} \\ c_{21} & c_{22} \end{pmatrix}, \quad (\text{A.1})$$

$$\rightarrow M(a_{ij}, c_{ij}) \begin{pmatrix} b_{11} \\ b_{12} \\ b_{21} \\ b_{22} \end{pmatrix} = M(a_{ij}, c_{ij}) B^c, \quad (\text{A.2})$$

where $M(a, c)$ is a matrix depending on the element of matrix A and C . We can directly calculate the multiplication to obtain

$$ABC = \begin{pmatrix} a_{11}b_{11}c_{11} + a_{12}b_{21}c_{11} & a_{11}b_{11}c_{12} + a_{12}b_{21}c_{12} \\ +a_{11}b_{12}c_{21} + a_{12}b_{22}c_{21} & +a_{11}b_{12}c_{21} + a_{12}b_{22}c_{21} \\ a_{21}b_{11}c_{11} + a_{22}b_{21}c_{11} & a_{21}b_{11}c_{12} + a_{21}b_{21}c_{12} \\ +a_{21}b_{12}c_{21} + a_{21}b_{22}c_{21} & +a_{21}b_{12}c_{21} + a_{21}b_{22}c_{21} \end{pmatrix}, \quad (\text{A.3})$$

comparing with Eq.(A.2), we can get

$$M(a_{ij}, c_{ij}) \begin{pmatrix} b_{11} \\ b_{12} \\ b_{21} \\ b_{22} \end{pmatrix} = \begin{pmatrix} a_{11}c_{11} & a_{11}c_{21} & a_{12}c_{11} & a_{12}c_{21} \\ a_{11}c_{12} & a_{11}c_{22} & a_{12}c_{12} & a_{12}c_{22} \\ a_{21}c_{11} & a_{21}c_{21} & a_{22}c_{11} & a_{22}c_{21} \\ a_{21}c_{12} & a_{21}c_{22} & a_{22}c_{12} & a_{22}c_{22} \end{pmatrix} \begin{pmatrix} b_{11} \\ b_{12} \\ b_{21} \\ b_{22} \end{pmatrix}. \quad (\text{A.4})$$

By observing Eq.(A.4), it is clear that $M(a_{ij}, c_{ij})$ is equal to $A \otimes C^T$. Where the symbol \otimes denotes a tensor product and C^T is the transpose of the matrix C . The matrix element of the multiplication of ABC can be written as $a_{ik}b_{kl}c_{lj}$. We can rewrite the resultant matrix element to $a_{ik}c_{lj}b_{kl}$. If we pick out the element b_{kl} to become a column, the elements a_{ik} and c_{lj} will construct a new square matrix, M . The character of the new matrix, M , is that the r -th row of MB^c should be the same as the element $(ABC)_{st}$, and r, s and t satisfy the condition

$$r = (s - 1) \times 2 + t. \quad (\text{A.5})$$

Therefore, if we have three multiplication $N \times N$ square matrix the condition becomes

$$r = (s - 1) \times N + t. \quad (\text{A.6})$$

Using Eq.(A.6) we obtain

$$M(a_{ij}, c_{ij}) = \begin{pmatrix} a_{11}c_{11} & a_{11}c_{21} & \dots & a_{11}c_{n1} & a_{12}c_{11} & \dots & a_{1n}c_{n1} \\ a_{11}c_{12} & a_{11}c_{22} & \dots & a_{11}c_{n2} & a_{12}c_{12} & \dots & a_{1n}c_{n2} \\ \vdots & \vdots & \vdots & \vdots & \vdots & \vdots & \vdots \\ a_{11}c_{1n} & a_{11}c_{2n} & \dots & a_{11}c_{nn} & a_{12}c_{1n} & \dots & a_{1n}c_{nn} \\ a_{21}c_{11} & a_{21}c_{21} & \dots & a_{21}c_{n1} & a_{22}c_{21} & \dots & a_{2n}c_{n1} \\ \vdots & \vdots & \vdots & \ddots & \vdots & \vdots & \vdots \\ a_{n1}c_{1n} & a_{n1}c_{2n} & \dots & a_{n1}c_{nn} & a_{n2}c_{nn} & \dots & a_{nn}c_{nn} \end{pmatrix}. \quad (\text{A.7})$$

We can further rewrite Eq.(A.7) in the following form

$$\begin{aligned}
& M \quad (a_{ij}, c_{ij}) \\
& = \left(\begin{array}{c} a_{11} \\ \vdots \\ a_{21} \\ \vdots \\ a_{n1} \end{array} \left(\begin{array}{cccc} c_{11} & c_{21} & \dots & c_{n1} \\ c_{12} & c_{22} & \dots & c_{n2} \\ \vdots & \vdots & \ddots & \vdots \\ c_{1n} & c_{2n} & \dots & c_{nn} \end{array} \right) \dots \left(\begin{array}{c} a_{1n} \\ \vdots \\ a_{2n} \\ \vdots \\ a_{nn} \end{array} \left(\begin{array}{cccc} c_{11} & c_{21} & \dots & c_{n1} \\ c_{12} & c_{22} & \dots & c_{n2} \\ \vdots & \vdots & \ddots & \vdots \\ c_{1n} & c_{2n} & \dots & c_{nn} \end{array} \right) \right) \\
& = A \otimes C^T. \tag{A.8}
\end{aligned}$$

Therefore, when the matrix B is changed to a column vector, we can use Eq.(A.8) to obtain equivalent result of ABC . Note that the column vector is arranged in the following way.

$$\left(\begin{array}{cccc} b_{11} & b_{12} & \dots & b_{1n} \\ b_{21} & b_{22} & \dots & b_{2n} \\ \vdots & \vdots & \ddots & \vdots \\ b_{n1} & b_{n2} & \dots & b_{nn} \end{array} \right) \Rightarrow \left(\begin{array}{c} b_{11} \\ b_{12} \\ \vdots \\ b_{1n} \\ b_{21} \\ \vdots \\ b_{nn} \end{array} \right). \tag{A.9}$$